STRUCTURAL CHEMISTRY
ISSN 2053-2296

Polymorphism of the dinuclear Co^{III}–Schiff base complex $[Co_2(o\text{-van-en})_3]\cdot 4CH_3CN$ (*o*-van-en is a salen-type ligand)

Anna Vráblová,[a,b]* Juraj Černák,[a] Larry R. Falvello[b,c] and Milagros Tomás[b,d]

[a]Department of Inorganic Chemistry, Institute of Chemistry, P. J. Šafárik University in Košice, Moyzesova 11, Košice, SK-04154, Slovakia, [b]Department of Inorganic Chemistry, University of Zaragoza, Pedro Cerbuna 12, Zaragoza, E-50009, Spain, [c]Aragón Materials Science Institute (ICMA), University of Zaragoza, Pedro Cerbuna 12, Zaragoza, E-50009, Spain, and [d]Institute of Chemical Synthesis and Homogeneous Catalysis (ISQCH), University of Zaragoza, Pedro Cerbuna 12, Zaragoza, E-50009, Spain. *Correspondence e-mail: anna.vrablova@student.upjs.sk

Received 17 January 2019
Accepted 1 March 2019

Edited by A. R. Kennedy, University of Strathclyde, Scotland

Keywords: dinuclear cobalt(III); crystal structure; polymorphism; full interaction map; Schiff base ligand.

CCDC references: 1900885; 1900884

Supporting information: this article has supporting information at journals.iucr.org/c

Reactions of $Co(OH)_2$ with the Schiff base bis(2-hydroxy-3-methoxybenzylidene)ethylenediamine, denoted H_2(*o*-van-en), under different conditions yielded the previously reported complex aqua[bis(3-methoxy-2-oxidobenzylidene)ethylenediamine]cobalt(II), $[Co(C_{18}H_{18}N_2O_4)(H_2O)]$, **1**, under anaerobic conditions and two polymorphs of [μ-bis(3-methoxy-2-oxidobenzylidene)ethylenediamine]bis{[bis(3-methoxy-2-oxidobenzylidene)ethylenediamine]cobalt(III)} acetonitrile tetrasolvate, $[Co_2(C_{18}H_{18}N_2O_4)_3]\cdot 4CH_3CN$, *i.e.* monoclinic **2** and triclinic **3**, in the presence of air. Both novel polymorphs were chemically and spectroscopically characterized. Their crystal structures are built up of centrosymmetric dinuclear $[Co_2(o\text{-van-en})_3]$ complex molecules, in which each Co^{III} atom is coordinated by one tetradentate dianionic *o*-van-en ligand in an uncommon bent fashion. The pseudo-octahedral coordination of the Co^{III} atom is completed by one phenolate O and one amidic N atom of the same arm of the bridging *o*-van-en ligand. In addition, the asymmetric units of both polymorphs contain two acetonitrile solvent molecules. The polymorphs differ in the packing orders of the dinuclear $[Co_2(o\text{-van-en})_3]$ complex molecules, *i.e.* alternating *ABABAB* in **2** and *AAA* in **3**. In addition, differences in the conformations, the positions of the acetonitrile solvent molecules and the pattern of intermolecular interactions were observed. Hirshfeld surface analysis permits a qualitative inspection of the differences in the intermolecular space in the two polymorphs. A knowledge-based study employing Full Interaction Maps was used to elucidate possible reasons for the polymorphism.

1. Introduction

Polymorphism in the crystalline state – 'the ability of a compound to crystallize in more than one crystal structure' (Cruz-Cabeza *et al.*, 2015) – is important from a scientific, as well as from an industrial, point of view as sometimes subtle differences in the crystal structures of the polymorphs may lead to substantially different properties. Such behaviour has been observed in the case of nonlinear optical materials (Munshi *et al.*, 2008), single molecule magnets (Pavlov *et al.*, 2016), materials with spin-crossover (Tao *et al.*, 2012) or gas-absorption properties (Pal *et al.*, 2016), or the properties of pharmaceutically active materials (Covaci *et al.*, 2017; Rodríguez-Spong *et al.*, 2004; Potticary *et al.*, 2016), to mention a few examples. Recently, progress in the prediction of the crystal structures of polymorphs using solid-state density functional theory (DFT) simulations has been reported (Hasnip *et al.*, 2014).

Schiff bases in their deprotonated forms are widely used ligands as they may exhibit several potential coordination

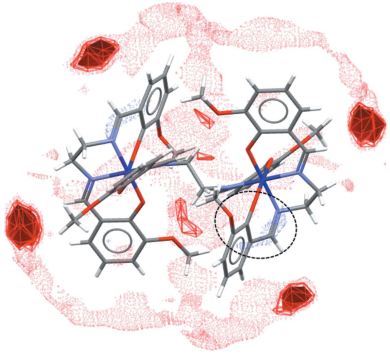

sites, which allows them to bond to one or more central metal atoms (Rezaeivala & Keypour, 2014; Vigato & Tamburini, 2004; Andruh, 2015). Reaction of ethane-1,2-diamine with *o*-vanillin in a 1:2 molar ratio results in a Schiff base of the salen type, namely bis(2-hydroxy-3-methoxybenzylidene)ethylenediamine, denoted H_2(*o*-van-en) (see Scheme 1). At present, more than 300 crystal structures, among them numerous complexes with transition metals and lanthanides (or their combinations), with this Schiff base are held in the Cambridge Structural Database (CSD; Groom *et al.*, 2016). Surprisingly, we find only one case for which polymorphism was reported, namely the copper complex [Cu(*o*-van-en)(H_2O)]. One polymorph of this compound [CSD refcodes WICBIU (Saha *et al.*, 2007) and WICBIU01 (Odabaşoğlu *et al.*, 2007)] crystallizes in the orthorhombic space group *Pnma* with $Z' = 1$, while the second crystallizes in the noncentrosymmetric orthorhombic space group $Pna2_1$ with $Z' = 3$ (refcode WICBIU02; Zhou *et al.*, 2015). It should be noted that the H_2(*o*-van-en) Schiff base itself forms two known polymorphs whose formation can be considered as a consequence of two possible conformations of the ethane-1,2-diamine part of the molecule. Molecules of H_2(*o*-van-en) with an *anti* conformation of the ethane-1,2-diamine fragment (VOJSUH; Cunningham *et al.*, 2004) crystallize in the monoclinic space group $P2_1/n$ (Cunningham *et al.*, 2004). In contrast, the polymorph crystallizing in the monoclinic space group *Pc* contains H_2(*o*-van-en) molecules with a *syn* arrangement of the ethane-1,2-diamine fragment [refcodes VOJSUI (Mo *et al.*, 1990) and VOJSUI02 (Correia *et al.*, 2005)].

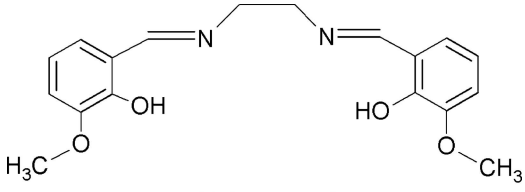

H_2(*o*-van-en)
Scheme 1

Within our broader study of Co^{II} complexes as magnetically active materials (Burzurí *et al.*, 2011; Smolko *et al.*, 2016), we have undertaken the study of the system formed by cobalt(II) hydroxide with the salen-type ligand *o*-van-en. From this system, depending on the experimental conditions, we have isolated three complexes, namely the previously reported [Co(*o*-van-en)(H_2O)] (**1**) and two novel polymorphs of [Co_2(*o*-van-en)$_3$]·4CH_3CN (**2** and **3**; see Scheme 2). The synthesis and crystal structure of **1** have already been reported (Jiang *et al.*, 2007). We report here a modified synthetic procedure leading to **1**, as well as the syntheses, crystal structures and comparisons of polymorphs **2** and **3**. We note that the analogous complex [Co_2(*o*-van-en)$_3$]·2Me_2SO·2H_2O with dimethyl sulfoxide and water solvent molecules (whose content was not fully stoichiometric), was previously prepared and structurally characterized from photographic data (Calligaris *et al.*, 1970).

In seeking the factors responsible for polymorphism in [Co_2(*o*-van-en)$_3$]·4CH_3CN, we undertook a study of the Full Interaction Maps (FIMs) for the two structures (Wood *et al.*, 2013). These permitted what we believe is a plausible explanation for the origin of the polymorphism in this compound.

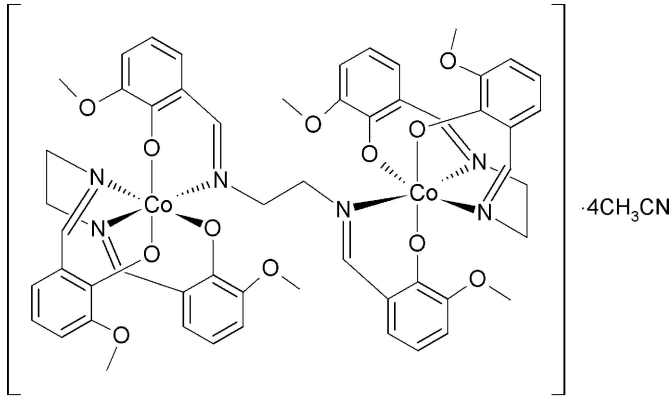

[Co_2(*o*-van-en)$_3$]·4MeCN, **2** and **3**
Scheme 2

2. Experimental

2.1. Materials

H_2(*o*-van-en) was synthesized using a slight modification of the procedure described by Ghose (1983, 1984), by the reaction of ethane-1,2-diamine and *o*-vanillin in a 1:2 molar ratio under reflux conditions in ethanol. The remaining chemicals were used as received from commercial sources.

2.2. Methods

Elemental analyses (C, H and N) were performed on a PerkinElmer 2400 Series II CHNS/O analyser. IR spectra were recorded on a PerkinElmer Spectrum 100 CsI DTGS FT–IR spectrometer with a UATR 1 bounce-KRS-5 in the range 4000–300 cm^{-1} (UATR is a universal attenuated total reflectance accessory and KRS-5 is thallium bromoiodide). The X-ray powder diffraction pattern of **1** was measured on a Rigaku D-Max/2500 diffractometer with a rotating anode and an RINT2000 vertical goniometer in the 2θ range 2.5–40° using Cu $K\alpha$ radiation ($\lambda = 1.54178$ Å) and a step size of 0.03°; the model powder diffraction pattern was calculated using the program *Mercury* (Macrae *et al.*, 2008).

For calculations of the Hirshfeld surfaces, the program *CrystalExplorer* was used (Spackman & Jayatilaka, 2009; Spackman & McKinnon, 2002). Full Interaction Maps (FIMs) (Wood *et al.*, 2013) were calculated using the program *Mercury* (Macrae *et al.*, 2008).

2.3. Synthesis and crystallization

2.3.1. [Co(*o*-van-en)(H_2O)], 1. Solid $Co(OH)_2$ (0.07 g, 0.76 mmol) was added to a deoxygenated water suspension of H_2(*o*-van-en) (0.25 g, 0.76 mmol, 35 ml) under an inert argon atmosphere at room temperature. An orange solid appeared after a few minutes of stirring. The mixture was stirred overnight and the final dark-orange microcrystalline product **1** was filtered off, washed with water and dried in air (yield 80%,

Table 1
Experimental details.

	2 (Form I)	**3** (Form II)
Crystal data		
Chemical formula	$[Co_2(C_{18}H_{18}N_2O_4)_3]\cdot4C_2H_3N$	$[Co_2(C_{18}H_{18}N_2O_4)_3]\cdot4C_2H_3N$
M_r	1261.10	1261.10
Crystal system, space group	Monoclinic, $P2_1/c$	Triclinic, $P\overline{1}$
Temperature (K)	100	100
a, b, c (Å)	12.4355 (3), 21.6501 (4), 11.9462 (3)	10.4971 (5), 11.6195 (5), 13.7158 (6)
α, β, γ (°)	90, 115.364 (4), 90	70.471 (4), 71.667 (4), 72.466 (4)
V (Å^3)	2906.25 (15)	1460.26 (13)
Z	2	1
Radiation type	Mo $K\alpha$	Mo $K\alpha$
μ (mm^{-1})	0.64	0.64
Crystal size (mm)	0.19 × 0.17 × 0.04	0.21 × 0.14 × 0.05
Data collection		
Diffractometer	Rigaku Xcalibur Sapphire3	Rigaku Xcalibur Sapphire3
Absorption correction	Multi-scan (*CrysAlis PRO*; Rigaku OD, 2015)	Multi-scan (*CrysAlis PRO*; Rigaku OD, 2015)
T_{min}, T_{max}	0.925, 1.000	0.835, 1.000
No. of measured, independent and observed $[I > 2\sigma(I)]$ reflections	24772, 6530, 4887	20710, 6041, 5192
R_{int}	0.061	0.039
$(\sin\theta/\lambda)_{max}$ (Å^{-1})	0.650	0.628
Refinement		
$R[F^2 > 2\sigma(F^2)]$, $wR(F^2)$, S	0.045, 0.106, 1.02	0.037, 0.094, 1.04
No. of reflections	6530	6041
No. of parameters	475	421
No. of restraints	0	3
H-atom treatment	H atoms treated by a mixture of independent and constrained refinement	H atoms treated by a mixture of independent and constrained refinement
$\Delta\rho_{max}$, $\Delta\rho_{min}$ (e Å^{-3})	0.54, −0.39	0.89, −0.35

Computer programs: *CrysAlis PRO* (Rigaku OD, 2015), *SHELXT2014* (Sheldrick, 2015*a*), *DIAMOND* (Brandenburg & Putz, 1999), *Mercury* (Macrae *et al.*, 2008), *SHELXL2018* (Sheldrick, 2015*b*), *WinGX* (Farrugia, 2012), *PARST* (Nardelli, 1983) and *CrystalExplorer* (Spackman & Jayatilaka, 2009).

based on Co). Elemental analysis (%) calculated for $C_{18}H_{20}CoN_2O_5$: C 53.61, H 5.00, N 6.95; found: C 53.80, H 4.88, N 6.87. IR (ν/cm^{-1}): 3315 (*b*), 3055 (*w*), 2899 (*w*), 2827 (*w*), 1651 (*m*), 1625 (*m*), 1600 (*m*), 1545 (*m*), 1468 (*m*), 1438 (*s*), 1391 (*m*), 1310 (*m*), 1239 (*s*), 1213 (*s*), 1169 (*m*), 1078 (*m*), 980 (*m*), 967 (*m*), 853 (*m*), 743 (*m*), 723 (*s*), 640 (*m*), 421 (*m*).

2.3.2. Monoclinic $[Co_2(o\text{-van-en})_3]\cdot4CH_3CN$ (Form I), 2. The microcrystalline product **1** was dissolved in acetonitrile in air with stirring at room temperature and after dissolution was left aside for crystallization. Within a few hours, the resulting solution had changed colour from dark red to brown–black. Black block-shaped crystals of **2** were obtained after a few days. As the crystals were unstable when separated from the mother liquor, presumably due to loss of solvent molecules, they were mounted for diffraction data collection immediately after removal from the mother liquor.

2.3.3. Triclinic $[Co_2(o\text{-van-en})_3]\cdot4CH_3CN$ (Form II), 3. Solid $Co(OH)_2$ (0.07 g, 0.76 mmol) was added to a water suspension of H_2(*o*-van-en) (0.25 g, 0.76 mmol, 20 ml) at room temperature in air and stirred overnight until the microcrystalline solid had changed colour from yellow–brown to black. The product thus formed was filtered off, dried in air and recrystallized from hot acetonitrile solution (~60–70 °C). Black block-shaped crystals of **3** appeared after a few days. The crystals of **3** were not stable in air, so they were mounted for diffraction data collection immediately after removal from the acetonitrile solution.

2.4. Refinement

Crystal data and global indicators from the structure refinements are collected in Table 1. For polymorph **2**, nonmethyl H atoms were located in a difference map and refined freely with individual variable isotropic displacement parameters. Methyl H atoms were initially placed at positions derived from difference electron-density maps, with C—H = 0.98 Å, and were refined as riders, with U_{iso}(H) = 1.5U_{eq} of their respective bonding partners; the methyl groups were allowed to rotate but not tilt. The disordered methyl group at C1 was split into two parts, both with half occupancy.

In polymorph **3**, the H atoms bonded to imine atoms C8, C11 and C26 were found in a difference map and refined freely. The remaining nonmethyl H atoms, as well as the methyl H atoms of the complex (at C1, C18 and C19), were placed at calculated positions (C—H = 0.99, 0.98 and 0.95 Å for methylene, methyl and aromatic H atoms, respectively). The methyl H atoms of the CH_3CN molecules were placed at positions derived from a difference map and refined as riders which were permitted to rotate but not tilt. The disordered MeCN molecule was split into two parts with occupancies constrained to sum to unity and with C—C and C—N bonds restrained to be the same lengths in both congeners. For the H atoms, U_{iso} values were set at xU_{eq} of their respective bonding partners, with x = 1.2 for nonmethyl H atoms and the methyl group at C28, and x = 1.5 for the remaining methyl groups.

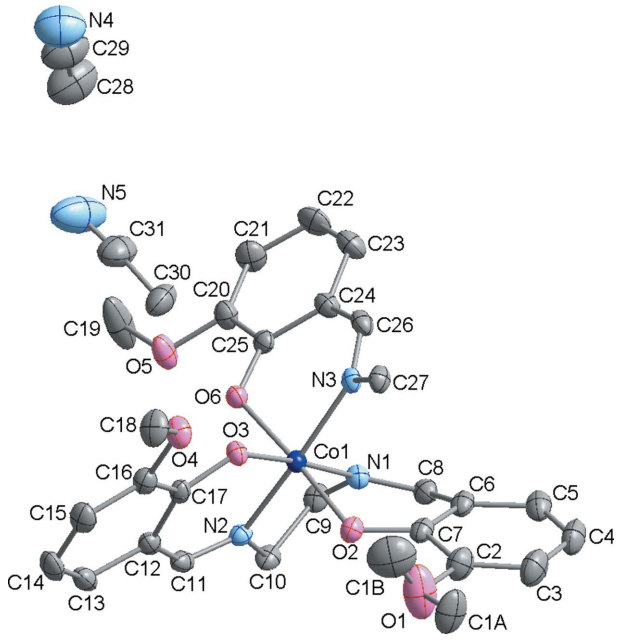

Figure 1
The asymmetric unit of **2**, with the atom-numbering scheme. Displacement ellipsoids are drawn at the 50% probability level. Half of the dinuclear molecule (without H atoms) is depicted for the sake of clarity.

3. Results and discussion

3.1. Syntheses and identification

Jiang *et al.* (2007) reported the crystal structure and the *in situ* solvothermal synthesis of the complex [Co(*o*-van-en)-(H_2O)], **1**, starting from 2-hydroxy-3-methoxybenzaldehyde, ethane-1,2-diamine and cobalt(II) nitrate. We have prepared the same product in microcrystalline form by direct reaction of cobalt(II) hydroxide with the Schiff base H_2(*o*-van-en) under mild conditions and an inert argon atmosphere. Le Bail refinement (Fig. S1 in the supporting information) of the measured X-ray diffraction pattern of **1** using the program *JANA2006* (Le Bail *et al.*, 1988; Petříček *et al.*, 2014) corroborated the phase purity and the identity of our product **1** with that reported by Jiang *et al.* (2007). In addition, the identity and the phase purity of **1** were further confirmed by the results of the elemental analysis.

An attempt to recrystallize microcrystalline product **1** from acetonitrile at room temperature in the presence of air led to oxidation of Co^{II} to Co^{III} and the formation of the monoclinic form (Form I, **2**) of [Co_2(*o*-van-en)$_3$]·4CH_3CN. Direct reaction of the Schiff base with $Co(OH)_2$ in the presence of air led to a black microcrystalline crude product, clearly indicating oxidation of the starting Co^{II} to Co^{III}. When the resulting crude product was recrystallized from hot acetonitrile, crystals of the triclinic form (Form II, **3**) of [Co_2(*o*-van-en)$_3$]·4CH_3CN separated out. We note that Calligaris *et al.* (1970) prepared single crystals of the analogous complex [Co_2(*o*-van-en)$_3$]·-2Me_2SO·2H_2O with dimethyl sulfoxide and water solvent molecules starting from the Co^{II} complex **1**.

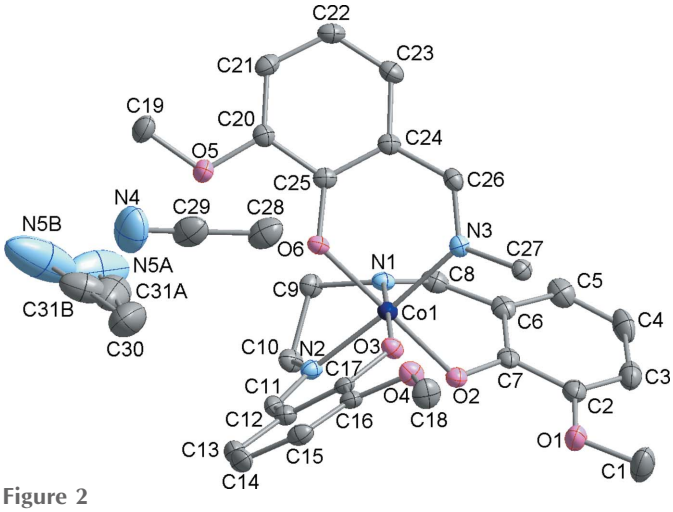

Figure 2
The asymmetric unit of **3**, with the atom-numbering scheme. Displacement ellipsoids are drawn at the 50% probability level. Only the half of the dinuclear molecule present in the asymmetric unit is drawn (without H atoms) for the sake of clarity.

Table 2
Selected bond lengths (Å) for **2** and **3**.

	2	**3**
Co1—O3	1.8915 (16)	1.8966 (13)
Co1—O2	1.9073 (17)	1.9002 (13)
Co1—O6	1.9093 (16)	1.9118 (13)
Co1—N1	1.8894 (19)	1.8993 (16)
Co1—N2	1.9041 (19)	1.9133 (16)
Co1—N3	1.9445 (19)	1.9271 (16)

3.2. Crystal structures

The molecular and crystal structure of **1** was reported by Jiang *et al.* (2007). The central Co^{II} atom in **1** is pentacoordinate, with the donor atoms from the Schiff base occupying the basal plane of the square pyramid, while the apical position is occupied by an aqua ligand (Fig. S2 in the supporting information).

Form I of [Co_2(*o*-van-en)$_3$]·4CH_3CN (polymorph **2**) crystallizes in the monoclinic space group $P2_1/c$, while Form II (polymorph **3**) crystallizes in the triclinic space group $P\overline{1}$. The crystal structures of both **2** and **3** are built up of centrosymmetric dinuclear [Co_2(*o*-van-en)$_3$] complex molecules; the triclinic form contains one dinuclear centrosymmetric molecule in the unit cell ($Z = 1$), while for the monoclinic form, $Z = 2$ (Figs. 1 and 2, respectively). In both polymorphs, the Co^{III} atoms are coordinated by one tetradentate *o*-van-en ligand in an uncommon bent fashion. A similar bent coordination was reported for [Fe_2(*o*-van-en)$_3$]·CH_2Cl_2·0.5H_2O (Costes *et al.*, 2010). The pseudo-octahedral coordination environments of the Co^{III} atoms are completed by one phenolate O and one imine N atom placed in *cis* positons and originating from the same arm of the bridging *o*-van-en ligand. In addition, the asymmetric units of both polymorphs contain two acetonitrile (MeCN) solvent molecules. The crystal structure of [Co_2(*o*-van-en)$_3$]·2Me_2SO·2H_2O (CSD refcode COMSAL; Calligaris *et al.*, 1970) contains the same complex molecule; the atomic

Table 3
Hydrogen-bond geometry (Å, °) for **2**.

D—H···A	D—H	H···A	D···A	D—H···A
C1B—H1BA···N4^{ii}	0.98	2.59	3.333 (10)	133
C1B—H1BB···O2	0.98	2.44	2.985 (8)	115
C8—H8···O5^{iii}	0.96 (3)	2.34 (3)	3.119 (3)	138 (2)
C9—H9B···O6	1.00 (3)	2.51 (2)	2.924 (3)	104.6 (17)
C27—H27A···O2	0.94 (2)	2.45 (2)	3.042 (3)	121.1 (18)
C27—H27B···O3^{i}	0.93 (3)	2.53 (2)	3.180 (3)	127.5 (18)
C28^{ii}—H28C^{ii}···O1	0.98	2.52	3.266 (5)	133
C30—H30C···O3	0.98	2.52	3.188 (3)	126
C30—H30C···O6	0.98	2.34	3.245 (3)	153

Symmetry codes: (i) $-x+1, -y+1, -z+1$; (ii) $x-1, y, z$; (iii) $x, -y+\frac{1}{2}, z+\frac{1}{2}$.

coordinates are not available for COMSAL, obviating a closer comparison with our two polymorphs.

The Co—O and Co—N bond lengths in **2** and **3** (see Table 2) are in line with those found for similar Co^{III} complexes, *e.g.* in [Co(salen)(acac)]·1.5H_2O (acac is acetyl acetate; Bailey *et al.*, 1972) and [Co(salen)(acac)]·0.7H_2O (Calligaris *et al.*, 1972). The values found are, as expected, somewhat shorter than those reported for Co^{II} complex **1**, in line with the smaller ionic radius of the Co^{III} atom (Shannon, 1976).

The dinuclear complex molecules in the two polymorphs display small but significant differences with respect to their geometrical parameters, and these can be clearly seen in Fig. 3. For example, the torsion angle O3—Co1—N2—C11 in Form I exhibits a value of 2.1 (2)°, in contrast to the corresponding value of 12.06 (19)° in Form II; as a consequence, the C12–C17 aromatic rings form different angles with the Co1/O3/N3/N1/N2 equatorial plane in the respective polymorphs, *i.e.* 6.89° in **2** *versus* 15.70° in **3** (Fig. S3 in the supporting information). As for the methoxy groups within the ligand, the most striking difference between Forms I and II is that in Form I, the O1 methoxy group is positionally disordered two ways, with occupancies set to half (Fig. 1). As for the remaining two methoxy groups, *i.e.* involving atoms O4 and O5, those with O5 display a small conformational difference in the two polymorphs, as can be seen by a comparison of the respective C19—O5—C20—C21 torsion angles, exhibiting values of 7.2 (4) (Form I) and 13.44 (1)° (Form II).

Packing diagrams for polymorphs **2** and **3** are shown in Fig. 4, in which the dinuclear [Co_2(*o*-van-en)$_3$] complex molecules are represented by CoO_3N_3 octahedra connected by four-atom centrosymmetric N3—C27—C27^{i}—N3^{i} bridges. The higher symmetry of Form I (monoclinic) coincides with a doubling of its unit-cell volume with respect to that of triclinic Form II. Moreover, the 2_1 screw axis parallel to *b* in Form I generates an alternating *ABABAB* stacking pattern, in

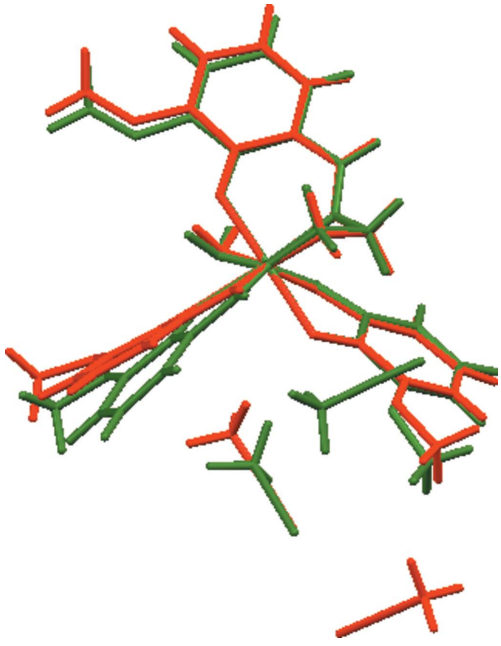

Figure 3
Wire models of the molecular structures of polymorphs **2** (red) and **3** (green). The structures are superimposed in such a way that the positions of the central Co atoms, as well as the donor atoms, are overlapped as nearly as possible. Only the asymmetric part of the dinuclear complex molecule is shown for clarity.

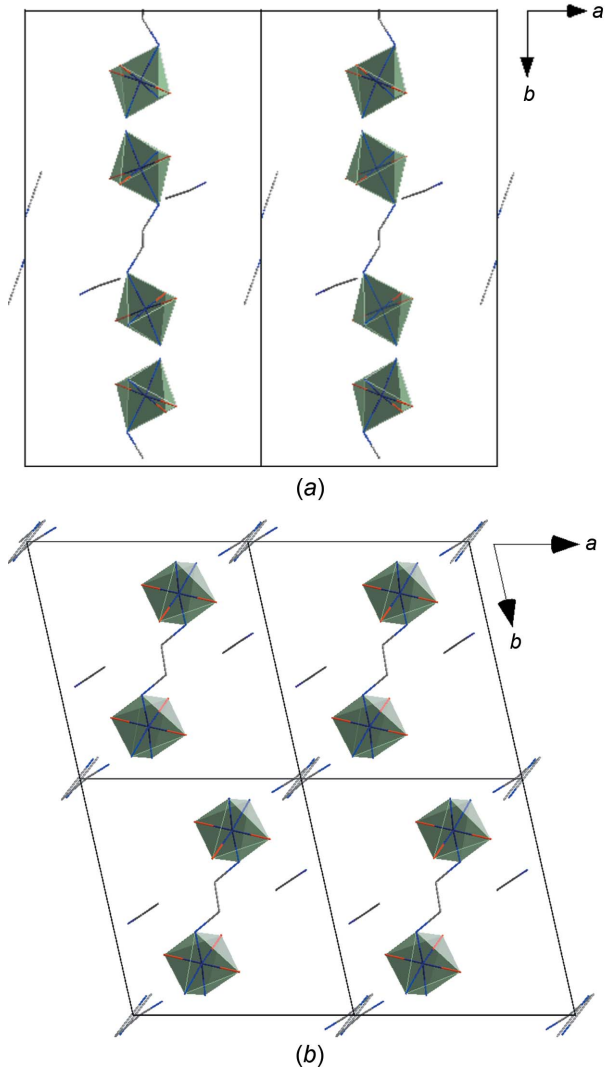

Figure 4
Packing in the crystal structures of (*a*) **2** and (*b*) **3**, each viewed along its *c* axis. For clarity, only coordination polyhedra, bridges linking the polyhedra and acetonitrile solvent molecules are shown.

Table 4
Hydrogen-bond geometry (Å, °) for **3**.

D—H···A	D—H	H···A	D···A	D—H···A
C5—H5···N5B^{iv}	0.95	2.57	3.454 (19)	156
C9—H9B···O6	0.99	2.50	2.955 (2)	107
C27—H27A···O3^{i}	0.99	2.50	3.148 (2)	123
C27—H27A···O4^{i}	0.99	2.56	3.463 (2)	151
C27—H27B···O2	0.99	2.40	2.980 (2)	117
C28—H28A···O6	0.98	2.29	3.256 (3)	169
C30—H30D···N4	0.98	2.56	3.451 (5)	151

Symmetry codes: (i) $-x+1, -y+1, -z+1$; (iv) $-x+2, -y, -z+1$.

contrast to Form II, in which the dinuclear units are arranged in a simple *AAA* manner. We note also that the MeCN solvent molecules occupy slightly different positions relative to the main molecules in the two polymorphs.

In what follows, we find it convenient to distinguish among hydrogen bonds of differing strengths and to treat these as distinct from contacts that may be adventitious and of questionable structure-directing capacity. For the purposes of this discussion, hydrogen bonds in which O and/or N atoms are both donors and acceptors will be called classical hydrogen bonds, those with imino or aromatic C—H groups as donors will be called nonclassical hydrogen bonds or weak hydrogen bonds and contacts involving methyl or methylene in donor roles will be called simply contacts, with no attempt at a more nuanced discrimination between what can and cannot be called a hydrogen bond. We will use a nonrigorous criterion, namely the default limits used by the program *PLATON* (Spek, 2009), to draw a convenient line between what we do and do not denote as hydrogen bonds – again, for the purposes of this discussion.

In both polymorphs, there are no classical hydrogen bonds due to the lack of suitable donors after deprotonation of the hydroxide groups. Surprisingly, among the weak hydrogen-bonding interactions of the =C—H···A or C_{ar}—H···A types (A = O or N), there is only one such hydrogen bond in each of the polymorphs, in both cases intermolecular.

In polymorph **2** (Form I), the only weak hydrogen-bonding interaction is C8—H8···O5^{iii} with participation of the imine H atom (see Table 3 for symmetry code). This interaction links the complex molecules into supramolecular layers in the *bc* plane (Fig. 5). The C11—H11 bond of the other imine group is directed toward the π-system of the C2^{iii}–C7^{iii} aromatic ring; this additional weak C—H···π interaction has an H···Cg distance of 2.91 (3) Å and a γ angle between the Cg—H vector and ring normal of 12.41°. As can be seen from Fig. 5, this interaction serves to reinforce the hydrogen-bonding interaction mentioned above. We note that additional intermolecular contacts of the C—H···X (X = N and O) type, with H atoms from the methoxy methyl group (C1B) or the MeCN solvent molecules (C28 and C30) can also be considered to contribute to the intermolecular cohesion (Table 3) and likewise for close contacts of the C—H···π type with participation of (C10—)H10 methylene and (C28—)H28A methyl H atoms (Table S1 in the supporting information). In Form I, there is no classical intramolecular hydrogen bonding, unless one

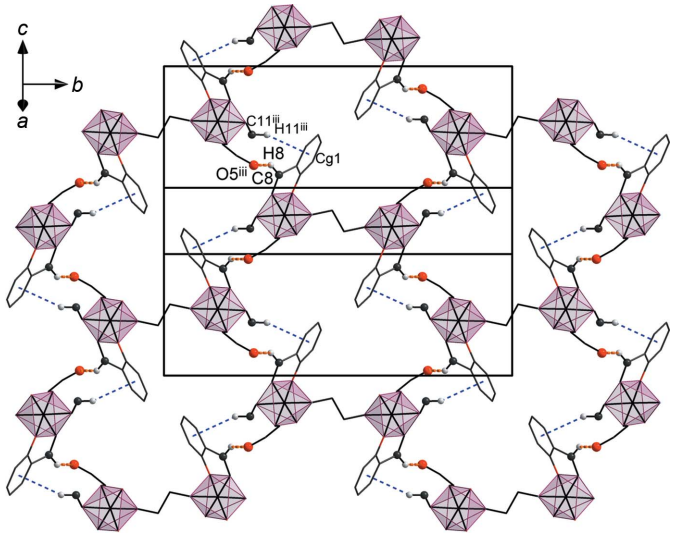

Figure 5
The supramolecular layer formed by weak intermolecular C—H···O hydrogen bonds (C8—H8···O5^{iii}; orange dashed lines) and C—H···π interactions (C11^{iii}—H11^{iii}···$Cg1$; blue dashed line) in **2**. The view is in the *bc* plane. $Cg1$ represents the centre of gravity of the C2–C7 aromatic ring. [Symmetry code: (iii) $x, -y+\frac{1}{2}, z+\frac{1}{2}$.]

considers close contacts of the C—H···O type with H atoms from a methoxy group (disordered C1 atom in position *B*) or methylene groups (C9 and C27; Table 3 and Fig. S4 in the supporting information) to be significant; these may help to stabilize the conformation of the complex molecule.

Similarly, in Form II, only one nonclassical hydrogen bond of the C_{ar}—H···N type, namely C5—H5···N5B^{iv} is present (Table 4 and Fig. 6) and this links the complex molecules with the disordered MeCN solvent molecule in the more populated position (N5*B*). As in Form I, there is one weak C—H···π interaction in which are involved the H21 atom from the aromatic ring as donor and the π-system of the C12^{v}–C17^{v}

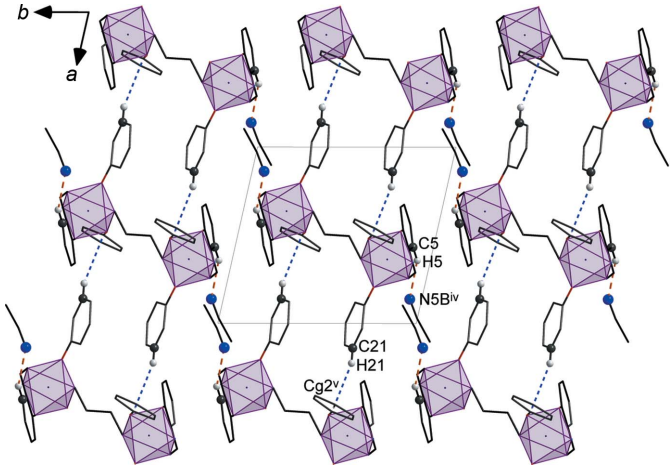

Figure 6
Packing mediated by the C5—H5···N5B^{iv} hydrogen bond (orange dashed line) and the $C21_{ar}$—H21···$Cg2^{v}$ interaction (blue dashed line) in **3**. $Cg2$ represents the centre of gravity of the C12–C17 aromatic ring. [Symmetry codes: (iv) $-x+2, -y, -z+1$; (v) $x+1, y, z$.]

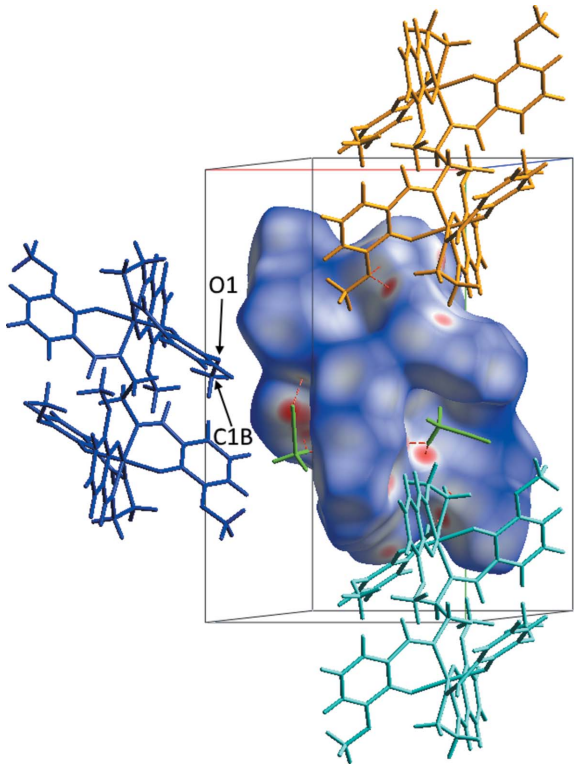

Figure 7
Hirshfeld surface of the dinuclear complex molecule of **2** plotted over d_{norm} (normalized contact distance) from −0.4000 to 1.5000 a.u., indicating the complex molecule with the disordered C1*B* methyl group in position *B*. The MeCN solvent molecules are displayed in green. Close contacts (O···H ≤ 2.60 Å and N···H ≤ 2.63 Å) are shown as red dashed lines. Neighbouring molecules are drawn using wire models in different colours in order to give a better view of the contacts.

aromatic ring as acceptor; the H···*Cg* distance is 2.64 Å and the γ angle between the *Cg*—H vector and the ring normal is 8.82°. This interaction links the complex molecules into supramolecular chains running along the *a* axis (Fig. 6). The crystal packing is also stabilized by additional contacts of the C—H···*X* (*X* = O and N) and C—H···π types coming from both MeCN solvent molecules and involving their methyl groups (Table 4) and the C9—H9*A* methylene group near the C20^{iv}–C25^{iv} aromatic ring (Table S2 in the supporting information). As for the intramolecular interactions, these include only contacts of the C—H···O type involving H atoms from methylene groups of the ligand (Table 4 and Fig. S5 in the supporting information).

With the aim of elucidating the factors responsible for the polymorphism of this system, we examined the packing patterns of structures **2** and **3** further using Hirshfeld surfaces (Spackman & Jayatilaka, 2009) and Full Interaction Maps (FIMs; Wood *et al.*, 2013).

The Hirshfeld surfaces for polymorphs **2** and **3** (Figs. 7 and 8, respectively) provide a concise visual indication that the intermolecular interactions are different in the two structures. In both cases, the structures suffer minor disorder, which complicates the preparation and interpretation of the Hirshfeld surfaces and fingerprint plots. This arises because the simultaneous presence of two disorder groups of the same disorder assembly will generate the appearance of artificial and impossibly short contacts in the Hirshfeld surfaces and fingerprint plots. At the same time, these tools do permit further discussion of the hydrogen bonds and other contacts. A full description and interpretation of the plots is given in the supporting information. We provide here only the aspects relevant to the present discussion.

Fig. 7 shows the Hirshfeld surface for one of the disordered congeners from structure **2** (for the second disordered congener, see Fig. S6 in the supporting information), for which no impossibly short contacts are generated. Fig. 8 shows an analogous plot for structure **3** (Fig. S7 gives the analogous plot for the second disordered congener of **3**). The distributions of favourable structure-stabilizing contacts (red areas) in the two plots give a clear qualitative indication that the intermolecular spaces in the two structures are organized in different fashions. This does not give us a clear indication of the origins of the polymorphism. To explore that question, we undertook an examination of FIMs.

The FIM (Wood *et al.*, 2013) is a knowledge-based tool that provides a visual map of the frequencies with which the chemical fragments or functional groups in a given structure have been observed to interact with different types of neighbours – for example, with hydrogen-bond donors or acceptors. The map is assembled using the crystal structure information held in the Cambridge Structural Database (Groom *et al.*, 2016), which as of this writing is approaching one million structures. We constructed the FIMs for structures **2** and **3** (Forms I and II, respectively) to see if indeed more than one possible favourable donor–acceptor set could be identified.

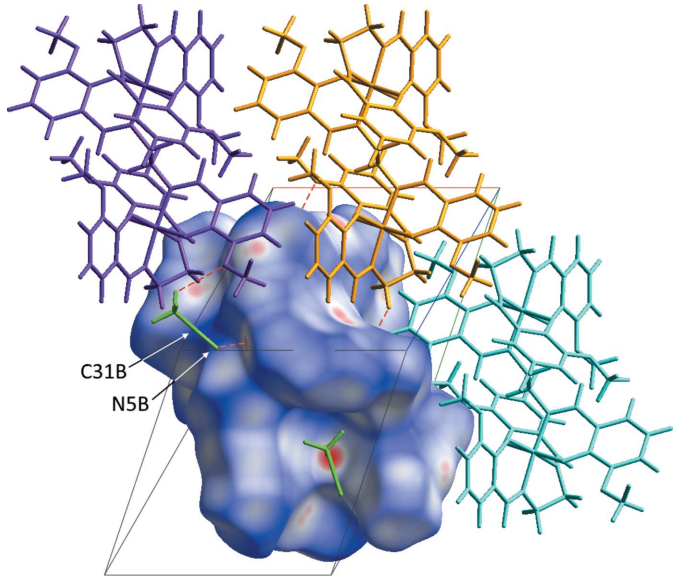

Figure 8
Hirshfeld surface diagram of the dinuclear complex molecule of **3** plotted over d_{norm} (normalized contact distance) from −0.4000 to 1.5000 a.u., indicating the disordered MeCN molecule in position *B*. The MeCN solvent molecules are displayed in green. Neighbouring complex molecules are shown in different colours using a wire model. Close contacts are displayed as red dashed lines, *i.e.* O···H ≤ 2.60 Å and N···H ≤ 2.63 Å.

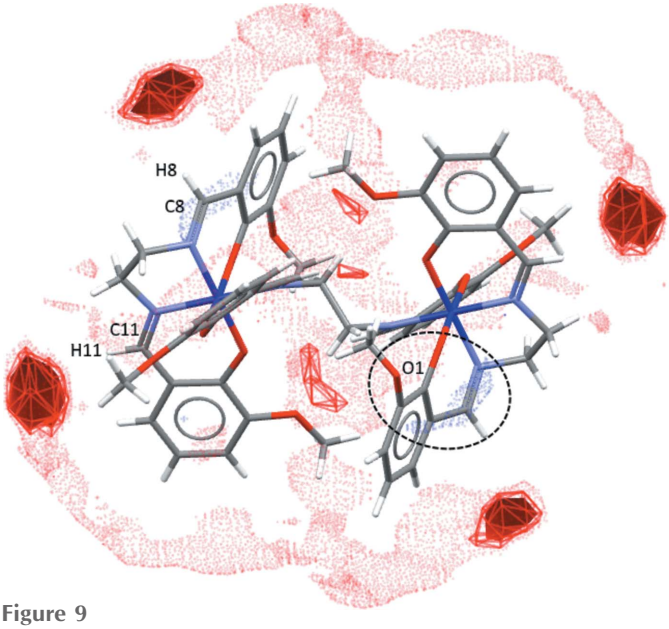

Figure 9
The FIM for complex molecules of **2**. Hydrogen-bond-donor regions are represented in blue and acceptor regions are represented in red. Dots, wireframe and solid regions represent frequencies of ×2, ×4 and ×6 those expected for a random distribution of contacts.

This would indicate that more than one arrangement of molecules in a crystal would produce stabilizing interactions.

The deprotonated H_2(*o*-van-en) molecule contains two potential donor sites at imine C atoms (Scheme 3, red arrows) and six acceptor sites (Scheme 3, blue arrows). Only two of the acceptor sites, namely the methoxy O atoms, are good candidates for intermolecular interactions, since the N atoms of the imine groups and the O atoms of the deprotonated hydroxy groups are occupied in coordination to the central Co^{III} atom.

For the FIM of polymorph **2**, we used only one disordered position of the methoxy group (atoms C1*B*, H1*BA*, H1*BB* and H1*BC*, with site-occupancy factors of 50%). The FIM displays four strong red (hydrogen-bond acceptor) regions, two of them symmetry independent (Fig. 9). They represent hydrogen-bond acceptors in the vicinity of the imine C—H group of the distal ligand. Furthermore, we observe a weak blue region near the potential acceptor site at methoxy atom O1 (circled in Fig. 9). The O atom of this orientation of the methoxy group is more exposed on the surface of the complex molecule, which is also reflected on the corresponding FIM (Fig. 9).

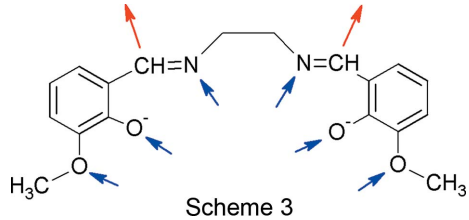

Scheme 3

In polymorph **2** (Form I), the acceptor region near the donor C11—H11 imine group, pictured in the FIM as a red region, is occupied by the electron density of the π-system of the C2^{iii}–C7^{iii} aromatic ring, and this contact, as described above, can be considered to be a weak C—H$\cdots\pi$ interaction [H$\cdots$*Cg* = 2.91 (3) Å and γ angle between *Cg*—H vector and ring normal of 12.41°; left circle in Fig. 10]. The acceptor region for the C8—H8 imine group is not occupied by any acceptor group (right circle in Fig. 10).

As seen for polymorph **2** (Form I), the FIM of the main molecule in polymorph **3** (Form II) shows four regions where the presence of hydrogen-bond acceptors is favoured, as observed in previously determined crystal structures (red regions in Fig. 11, two per asymmetric unit), reflecting the donor capabilities of the imine C8—H8 and C11—H11 groups and their symmetry relatives. The only possible acceptor sites (methoxy and oxy groups) are oriented toward the interior of the complex molecule, mostly forming intramolecular interactions, so that the FIM does not show any potential donor region.

In polymorph **3**, the donor C8—H8 imine group is involved in a rather weak intermolecular close contact (C8—H8$\cdots$O5^{iv};

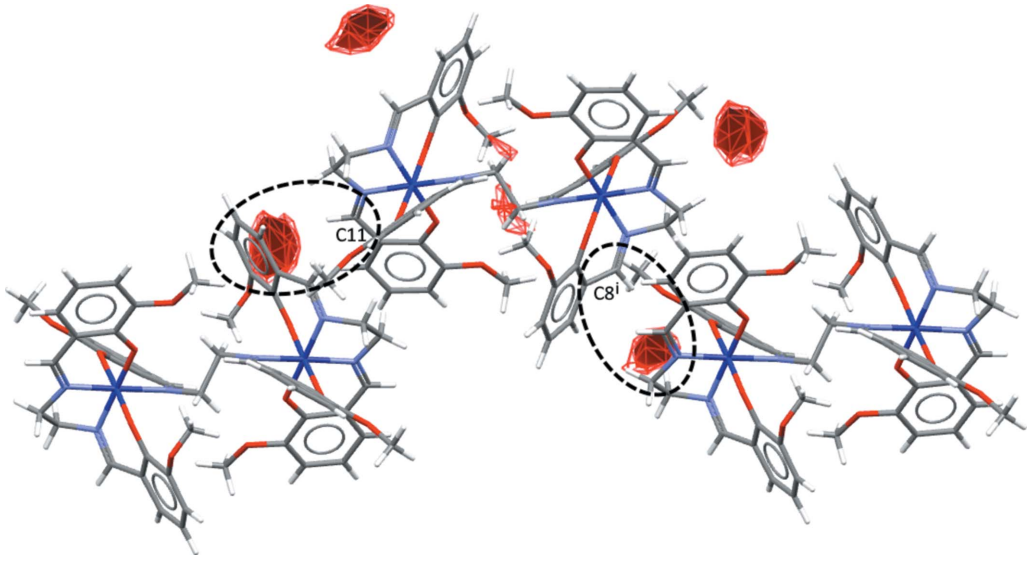

Figure 10
The environments of the two symmetrically independent donor regions in the FIM of polymorph **2**. Only the ×4 and ×6 levels are shown.

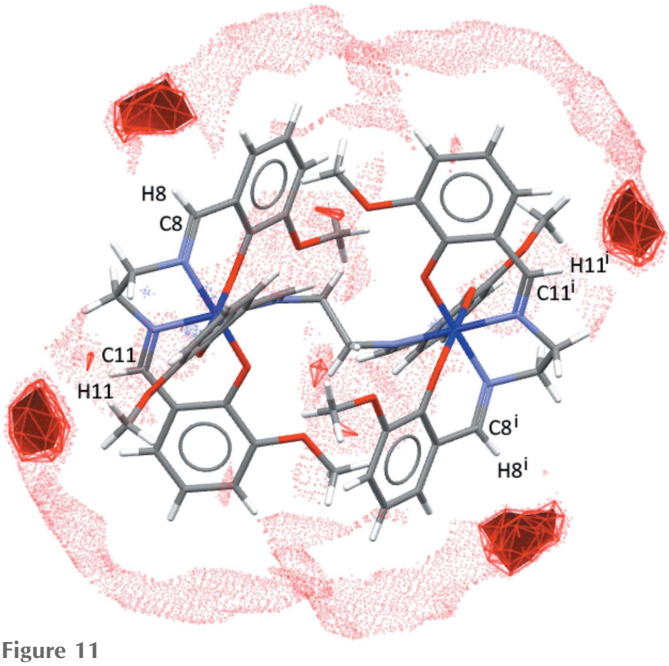

Figure 11
The FIM for complex molecules of polymorph **3**. Hydrogen-bond-donor regions are represented in blue and acceptor regions are represented in red. Dots, wireframe and solid regions represent frequencies of ×2, ×4 and ×6 those expected for a random distribution of contacts.

left circled interaction in Fig. 12), beyond the default limits of *PLATON* (Spek, 2009), and similarly, the donor site at the C11—H11 imine group is involved in a weak C—H···π interaction (right circled interaction in Fig. 12), also beyond the conventional limits of most programs. It is suggested that these interactions, weak though they be, act as directors for the packing of complex molecules in the structure of **3**.

In general, in **2** and **3**, the strongest regions of intermolecular interactions in the FIMs are occupied by symmetry-related molecules mediated by C—H···O-type hydrogen bonds and C—H···π interactions – or not occupied at all. None of the interactions mentioned lies exactly in the interaction region (the acceptor is too far away). MeCN molecules do not enter the donor or acceptor regions of the complex molecules in either of these two polymorphs.

The FIMs suggest that this molecule does not possess a strong capacity for self-recognition with significant interactions. In the configurations found in Forms I and II, four regions with a significant capacity for hydrogen-bond donation are not matched by any segments with the corresponding capacity to accept hydrogen bonds. So the polymorphism is not a result of a surfeit of molecular arrangements leading to highly stabilizing interactions. Rather, we conclude that the cohesion in the crystals of **2** and **3** is a result of energetically poorer interactions. And it is not surprising that there would be more than one way to achieve a lesser level of stability. We note again here that crystals of both polymorphs are unstable outside of their mother liquids at the temperature at which they are formed.

4. Conclusion

From the system $Co(OH)_2$ + H_2(*o*-van-en) under different experimental conditions, two cobalt complexes were isolated in a total of three solid forms – under anaerobic conditions, the already structurally characterized Co^{II} complex **1**, and in the presence of air, two novel Co^{III}-containing solids **2** and **3**. The new complexes were chemically and spectroscopically characterized. Products **2** and **3** are monoclinic and triclinic polymorphs, respectively, and both are formed by centrosymmetric dinuclear [Co_2(*o*-van-en)$_3$] complex molecules in which two tetradentate *o*-van-en ligands chelate the two hexacoordinated Co^{III} atoms, while the remaining *o*-van-en ligand bridges the two Co^{III} atoms in a bis-chelate fashion. The composition of both polymorphs is completed by two MeCN solvent molecules. The two polymorphs differ in the packing of the dinuclear [Co_2(*o*-van-en)$_3$] complex molecules and conformational differences in the complex molecules were also observed. The Hirshfeld surfaces reflect the observed disorder for both polymorphs and suggest possible reasons for it; they also confirm the presence of contacts represented by weak hydrogen-bonding interactions, and they further indicate that the MeCN molecules play a role in the packing as they fill the hollows formed between the packed complex molecules. The FIMs of both polymorphs show that the regions of intermolecular interactions are occupied by congeners of the complex, leaving unrequited hydrogen-bonding capability and suggesting an explanation for the polymorphism. Furthermore, acetonitrile solvent molecules as rich electron donors do

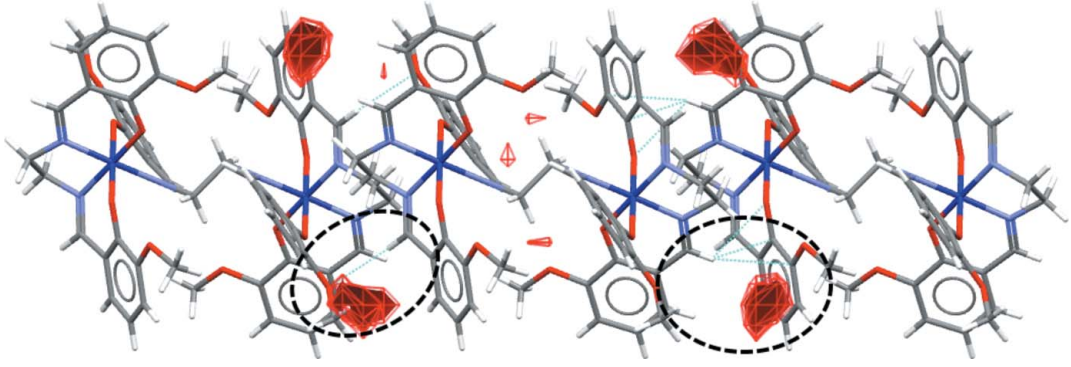

Figure 12
The occupation of two symmetrically independent donor regions in the FIM of polymorph **3**. Only ×4 and ×6 levels are shown.

not enter the acceptor regions of the complex in either of the two polymorphs. These observations corroborate the observed low stability of both polymorphs with respect to the loss of their solvent molecules.

Acknowledgements

AV thanks the National Scholarship Programme of the Slovak Republic for financing her study stay at the University of Zaragoza. This work benefitted from services provided by the Servicio General de Apoyo a la Investigación, University of Zaragoza.

Funding information

Funding for this research was provided by: Vedecká Grantová Agentúra (grant No. 1/0063/17); Agentúra na Podporu Výskumu a Vývoja (grant No. APVV-14-0078); Univerzita Pavla Jozefa Šafárika v Košiciach (Slovakia) (grant No. VVGS-PF-2018-777); Ministerio de Economía y Competitividad (grant No. MAT2015-68200-C2-1-P); European FEDER funds; Diputación General de Aragón (Project M4, E11_17R).

References

Andruh, M. (2015). *Dalton Trans.* **44**, 16633–16653.
Bailey, N. A., Higson, B. M. & McKenzie, E. D. (1972). *J. Chem. Soc. Dalton Trans.* pp. 503–508.
Brandenburg, K. & Putz, H. (1999). *DIAMOND*. Crystal Impact GbR, Bonn, Germany.
Burzurí, E., Campo, J., Falvello, L. R., Forcén-Vázquez, E., Luis, F., Mayoral, I., Palacio, F., Sáenz de Pipaón, C. & Tomás, M. (2011). *Chem. Eur. J.* **17**, 2818–2822.
Calligaris, M., Manzini, G., Nardin, G. & Randaccio, L. (1972). *J. Chem. Soc. Dalton Trans.* pp. 543–547.
Calligaris, M., Nardin, G. & Randaccio, L. (1970). *J. Chem. Soc. D*, **17**, 1079–1080.
Correia, I., Pessoa, J. C., Duarte, M. T., da Piedade, M. F. M., Jackush, T. C. A., Kiss, T., Castro, M. M. C. A., Geraldes, C. F. G. C. & Avecilla, F. (2005). *Eur. J. Inorg. Chem.* pp. 732–744.
Costes, J.-P., Dahan, F., Dumestre, F. & Tuchagues, J. (2010). *Polyhedron*, **29**, 787–790.
Covaci, O. I., Mitran, R. A., Buhalteanu, L., Dumitrescu, D. G., Shova, S. & Manta, C. (2017). *CrystEngComm*, **19**, 3584–3591.
Cruz-Cabeza, A. J., Reutzel-Edens, S. M. & Bernstein, J. (2015). *Chem. Soc. Rev.* **44**, 8619–8635.
Cunningham, D., Gilligan, K., Hannon, M., Kelly, C., McArdle, P. & O'Malley, A. (2004). *Organometallics*, **23**, 984–994.
Farrugia, L. J. (2012). *J. Appl. Cryst.* **45**, 849–854.
Ghose, B. N. (1983). *Rev. Port. Quim.* **28**, 147–150.
Ghose, B. N. (1984). *J. Chem. Eng. Data*, **29**, 237.
Groom, C. R., Bruno, I. J., Lightfoot, M. P. & Ward, S. C. (2016). *Acta Cryst.* B**72**, 171–179.
Hasnip, P. J., Refson, K., Probert, M. I. J., Yates, J. R., Clark, S. J. & Pickard, C. J. (2014). *Philos. Trans. Roy. Soc. A*, **372**, 20130270.
Jiang, G.-B., Zhang, S.-H. & Zeng, M.-H. (2007). *Acta Cryst.* E**63**, m2383.
Le Bail, A., Duroy, H. & Fourquet, J. L. (1988). *Mater. Res. Bull.* **23**, 447–452.
Macrae, C. F., Bruno, I. J., Chisholm, J. A., Edgington, P. R., McCabe, P., Pidcock, E., Rodriguez-Monge, L., Taylor, R., van de Streek, J. & Wood, P. A. (2008). *J. Appl. Cryst.* **41**, 466–470.
Mo, Y., Yang, G., Zhao, G. & Li, B. (1990). *Jilin Daxue Ziran Kex. Xue. (Chin.) (Acta Sci. Nat. Univ. Jil.)*, 93-1.
Munshi, P., Skelton, B. W., McKinnon, J. J. & Spackman, M. A. (2008). *CrystEngComm*, **10**, 197–206.
Nardelli, M. (1983). *Comput. Chem.* **7**, 95–98.
Odabaşoğlu, M., Arslan, F., Ölmez, H. & Büyükgüngör, O. (2007). *Dyes Pigments*, **75**, 507–515.
Pal, A., Chand, S., Senthilkumar, S., Neogi, S. & Das, M. C. (2016). *CrystEngComm*, **18**, 4323–4335.
Pavlov, A. A., Nelyubina, Y. V., Kats, S. V., Penkova, L. V., Efimov, N. N., Dmitrienko, O. A., Vologzhanina, A. V., Belov, A. S., Voloshin, Y. Z. & Novikov, V. V. (2016). *J. Phys. Chem. Lett.* **7**, 4111–4116.
Petříček, V., Dušek, M. & Palatinus, L. (2014). *Z. Kristallogr.* **229**, 345–352.
Potticary, J., Terry, L. R., Bell, C., Papanikolopoulos, A. N., Christianen, P. C. M., Engelkamp, H., Collins, A. M., Fontanesi, C., Kociok-Koehn, G., Crampin, S., Da Como, E. & Hall, S. R. (2016). *Nat. Commun.* **7**, article No. 11555.
Rezaeivala, M. & Keypour, H. (2014). *Coord. Chem. Rev.* **280**, 203–253.
Rigaku OD (2015). *CrysAlis PRO*. Rigaku Oxford Diffraction Ltd, Yarnton, Oxfordshire, England.
Rodríguez-Spong, B., Price, C. P., Jayasankar, A., Matzger, A. J. & Rodríguez-Hornedo, N. (2004). *Adv. Drug Deliv. Rev.* **56**, 241–274.
Saha, P. K., Dutta, B., Jana, S., Bera, R., Saha, S., Okamoto, K. & Koner, S. (2007). *Polyhedron*, **26**, 563–571.
Shannon, R. D. (1976). *Acta Cryst.* A**32**, 751–767.
Sheldrick, G. M. (2015*a*). *Acta Cryst.* A**71**, 3–8.
Sheldrick, G. M. (2015*b*). *Acta Cryst.* C**71**, 3–8.
Smolko, L., Černák, J., Kuchár, J., Miklovič, J. & Boča, R. (2016). *J. Mol. Struct.* **1119**, 437–441.
Spackman, M. A. & Jayatilaka, D. (2009). *CrystEngComm*, **11**, 19–32.
Spackman, M. A. & McKinnon, J. J. (2002). *CrystEngComm*, **4**, 378–392.
Spek, A. L. (2009). *Acta Cryst.* D**65**, 148–155.
Tao, J., Wei, R. J., Huang, R. B. & Zheng, L. S. (2012). *Chem. Soc. Rev.* **41**, 703–737.
Vigato, P. A. & Tamburini, S. (2004). *Coord. Chem. Rev.* **248**, 1717–2128.
Wood, P. A., Olsson, T. S. G., Cole, J. C., Cottrell, S. J., Feeder, N., Galek, P. T. A., Groom, C. R. & Pidcock, E. (2013). *CrystEngComm*, **15**, 65–72.
Zhou, H., Chen, C., Liu, Y. & Shen, X. (2015). *Inorg. Chim. Acta*, **437**, 188–194.

supporting information

Acta Cryst. (2019). C**75**, 433-442 [https://doi.org/10.1107/S2053229619003115]

Polymorphism of the dinuclear Co^{III}–Schiff base complex $[Co_2(o\text{-van-en})_3]\cdot 4CH_3CN$ (*o*-van-en is a salen-type ligand)

Anna Vráblová, Juraj Černák, Larry R. Falvello and Milagros Tomás

Computing details

For both structures, data collection: *CrysAlis PRO* (Rigaku OD, 2015); cell refinement: *CrysAlis PRO* (Rigaku OD, 2015); data reduction: *CrysAlis PRO* (Rigaku OD, 2015). Program(s) used to solve structure: SHELXT2014 (Sheldrick, 2015a) for (2); SHELXT (Sheldrick, 2015a) for (3). For both structures, program(s) used to refine structure: *SHELXL2018* (Sheldrick, 2015b); molecular graphics: *DIAMOND* (Brandenburg & Putz, 1999) and *Mercury* (Macrae *et al.*, 2008); software used to prepare material for publication: *SHELXL2018* (Sheldrick, 2015b), *WinGX* (Farrugia, 2012), *PARST* (Nardelli, 1983), *Mercury* (Macrae *et al.*, 2008) and CrystalExplorer (Spackman & Jayatilaka, 2009).

{*μ*-6,6′-Dimethoxy-2,2′-[ethane-1,2-diylbis(nitrilomethylylidene)]diphenolato}bis({6,6′-dimethoxy-2,2′-[ethane-1,2-diylbis(nitrilomethylylidene)]diphenolato}cobalt(III)) acetonitrile tetrasolvate (2)

Crystal data

$[Co_2(C_{18}H_{18}N_2O_4)_3]\cdot 4C_2H_3N$
M_r = 1261.10
Monoclinic, $P2_1/c$
a = 12.4355 (3) Å
b = 21.6501 (4) Å
c = 11.9462 (3) Å
β = 115.364 (4)°
V = 2906.25 (15) Å^3
Z = 2
$F(000)$ = 1316
D_x = 1.441 Mg m^{-3}
Mo $K\alpha$ radiation, λ = 0.71073 Å
Cell parameters from 7574 reflections
θ = 2.6–27.9°
μ = 0.64 mm^{-1}
T = 100 K
Block, black
0.19 × 0.17 × 0.04 mm

Data collection

Rigaku Xcalibur Sapphire3 diffractometer
Radiation source: fine-focus sealed X-ray tube
Detector resolution: 16.0655 pixels mm^{-1}
ω scans
Absorption correction: multi-scan (CrysAlis PRO; Rigaku OD, 2015)
T_{min} = 0.925, T_{max} = 1.000
24772 measured reflections
6530 independent reflections
4887 reflections with $I > 2\sigma(I)$
R_{int} = 0.061
θ_{max} = 27.5°, θ_{min} = 2.6°
h = −10→16
k = −28→28
l = −15→15

Refinement

Refinement on F^2
Least-squares matrix: full
$R[F^2 > 2\sigma(F^2)]$ = 0.045
$wR(F^2)$ = 0.106
S = 1.02
6530 reflections
475 parameters
0 restraints
Hydrogen site location: mixed

H atoms treated by a mixture of independent and constrained refinement
$w = 1/[\sigma^2(F_o^2) + (0.0415P)^2 + 2.4191P]$ where $P = (F_o^2 + 2F_c^2)/3$

$(\Delta/\sigma)_{max} = 0.001$
$\Delta\rho_{max} = 0.54$ e Å^{-3}
$\Delta\rho_{min} = -0.39$ e Å^{-3}

Special details

Geometry. All esds (except the esd in the dihedral angle between two l.s. planes) are estimated using the full covariance matrix. The cell esds are taken into account individually in the estimation of esds in distances, angles and torsion angles; correlations between esds in cell parameters are only used when they are defined by crystal symmetry. An approximate (isotropic) treatment of cell esds is used for estimating esds involving l.s. planes.

Fractional atomic coordinates and isotropic or equivalent isotropic displacement parameters (Å^2)

	x	*y*	*z*	U_{iso}*/U_{eq}	Occ. (<1)
Co1	0.48831 (3)	0.34589 (2)	0.52332 (3)	0.01690 (10)	
C1A	0.0959 (6)	0.4786 (3)	0.5548 (6)	0.0465 (17)	0.5
H1AA	0.054068	0.465902	0.604291	0.070*	0.5
H1AB	0.038800	0.482439	0.467709	0.070*	0.5
H1AC	0.134796	0.518532	0.584770	0.070*	0.5
C1B	0.1753 (7)	0.4687 (4)	0.4860 (8)	0.066 (2)	0.5
H1BA	0.093145	0.470064	0.421929	0.099*	0.5
H1BB	0.227948	0.454394	0.449458	0.099*	0.5
H1BC	0.199672	0.510176	0.520626	0.099*	0.5
O1	0.1815 (2)	0.43447 (13)	0.5655 (2)	0.0625 (8)	
C2	0.2813 (3)	0.42680 (13)	0.6732 (3)	0.0338 (6)	
C3	0.2922 (3)	0.45085 (14)	0.7843 (3)	0.0397 (7)	
H3	0.231 (3)	0.4759 (16)	0.787 (3)	0.058 (10)*	
C4	0.3971 (3)	0.44282 (13)	0.8922 (3)	0.0354 (7)	
H4	0.401 (3)	0.4622 (15)	0.972 (3)	0.046 (9)*	
C5	0.4882 (3)	0.40802 (12)	0.8898 (3)	0.0306 (6)	
H5	0.559 (2)	0.4004 (12)	0.958 (3)	0.026 (7)*	
C6	0.4769 (2)	0.38077 (11)	0.7776 (2)	0.0241 (5)	
C7	0.3751 (2)	0.39147 (11)	0.6662 (2)	0.0225 (5)	
O2	0.35797 (15)	0.36873 (8)	0.55871 (15)	0.0219 (4)	
C8	0.5531 (2)	0.33026 (11)	0.7801 (2)	0.0233 (5)	
H8	0.589 (2)	0.3067 (12)	0.855 (3)	0.027 (7)*	
N1	0.56198 (18)	0.31008 (9)	0.68266 (18)	0.0195 (4)	
C9	0.5917 (2)	0.24494 (11)	0.6753 (2)	0.0232 (5)	
H9A	0.611 (2)	0.2239 (11)	0.751 (2)	0.013 (6)*	
H9B	0.658 (2)	0.2407 (12)	0.650 (2)	0.024 (7)*	
C10	0.4759 (2)	0.21916 (11)	0.5771 (2)	0.0226 (5)	
H10A	0.419 (2)	0.2136 (11)	0.609 (2)	0.017 (6)*	
H10B	0.490 (2)	0.1813 (14)	0.547 (3)	0.031 (8)*	
N2	0.42731 (17)	0.26460 (9)	0.47585 (18)	0.0183 (4)	
C11	0.3560 (2)	0.24757 (11)	0.3665 (2)	0.0219 (5)	
H11	0.334 (2)	0.2048 (12)	0.351 (2)	0.019 (6)*	
C12	0.3033 (2)	0.28726 (11)	0.2601 (2)	0.0207 (5)	
C13	0.2252 (2)	0.26006 (13)	0.1463 (2)	0.0256 (6)	
H13	0.208 (2)	0.2190 (13)	0.137 (2)	0.023 (7)*	

C14	0.1697 (2)	0.29552 (13)	0.0424 (3)	0.0302 (6)
H14	0.121 (2)	0.2775 (12)	−0.031 (3)	0.023 (7)*
C15	0.1887 (2)	0.35921 (13)	0.0484 (2)	0.0287 (6)
H15	0.150 (2)	0.3825 (12)	−0.019 (3)	0.023 (7)*
C16	0.2658 (2)	0.38702 (12)	0.1567 (2)	0.0229 (5)
C17	0.3286 (2)	0.35149 (11)	0.2669 (2)	0.0193 (5)
O3	0.40290 (14)	0.38068 (7)	0.36424 (14)	0.0193 (4)
O4	0.29081 (16)	0.44881 (8)	0.17092 (15)	0.0274 (4)
C18	0.2169 (3)	0.48860 (13)	0.0722 (2)	0.0341 (7)
H18A	0.133467	0.482595	0.056156	0.051*
H18B	0.227127	0.478764	−0.002760	0.051*
H18C	0.239595	0.531694	0.095571	0.051*
C19	0.8545 (3)	0.2040 (2)	0.4522 (4)	0.0722 (14)
H19A	0.905411	0.183047	0.529613	0.108*
H19B	0.903669	0.229573	0.424754	0.108*
H19C	0.811829	0.173137	0.388512	0.108*
O5	0.77077 (16)	0.24213 (9)	0.47211 (17)	0.0340 (5)
C20	0.8141 (2)	0.29142 (12)	0.5507 (2)	0.0256 (6)
C21	0.9332 (2)	0.30292 (14)	0.6218 (3)	0.0333 (6)
H21	0.988 (3)	0.2788 (13)	0.619 (3)	0.033 (8)*
C22	0.9699 (3)	0.35454 (14)	0.6991 (3)	0.0346 (7)
H22	1.055 (3)	0.3626 (14)	0.744 (3)	0.042 (9)*
C23	0.8876 (2)	0.39446 (13)	0.7034 (3)	0.0308 (6)
H23	0.909 (3)	0.4306 (14)	0.749 (3)	0.040 (9)*
C24	0.7647 (2)	0.38375 (11)	0.6321 (2)	0.0231 (5)
C25	0.7256 (2)	0.33161 (11)	0.5540 (2)	0.0194 (5)
O6	0.61326 (14)	0.31951 (7)	0.48183 (14)	0.0194 (4)
C26	0.6809 (2)	0.43104 (11)	0.6263 (2)	0.0231 (5)
H26	0.715 (2)	0.4695 (12)	0.656 (2)	0.019 (6)*
N3	0.56686 (18)	0.42527 (9)	0.57678 (17)	0.0187 (4)
C27	0.4988 (3)	0.48305 (11)	0.5554 (2)	0.0215 (5)
H27A	0.420 (2)	0.4742 (11)	0.541 (2)	0.012 (6)*
H27B	0.531 (2)	0.5081 (11)	0.625 (2)	0.014 (6)*
N4	0.9999 (3)	0.45617 (16)	0.1839 (4)	0.0739 (10)
C28	1.0626 (4)	0.35371 (18)	0.3105 (4)	0.0734 (12)
H28A	1.078686	0.321934	0.261269	0.110*
H28B	0.998237	0.339792	0.331095	0.110*
H28C	1.134572	0.360997	0.387040	0.110*
C29	1.0272 (4)	0.41118 (19)	0.2390 (4)	0.0634 (11)
N5	0.7624 (3)	0.37794 (16)	0.2062 (4)	0.0865 (13)
C30	0.5962 (3)	0.41484 (14)	0.2652 (3)	0.0425 (8)
H30A	0.525967	0.424862	0.188793	0.064*
H30B	0.621204	0.451469	0.318414	0.064*
H30C	0.576697	0.381481	0.308818	0.064*
C31	0.6908 (3)	0.39542 (15)	0.2354 (3)	0.0498 (9)

Atomic displacement parameters (Å²)

	U^{11}	U^{22}	U^{33}	U^{12}	U^{13}	U^{23}
Co1	0.02012 (17)	0.01519 (16)	0.01537 (16)	0.00033 (13)	0.00758 (13)	0.00032 (13)
C1A	0.040 (4)	0.061 (4)	0.039 (3)	0.029 (3)	0.018 (3)	0.003 (3)
C1B	0.047 (5)	0.070 (5)	0.075 (6)	0.015 (4)	0.021 (4)	0.015 (5)
O1	0.0545 (16)	0.0705 (18)	0.0460 (15)	0.0338 (14)	0.0058 (13)	−0.0111 (13)
C2	0.0377 (17)	0.0335 (15)	0.0337 (15)	0.0073 (13)	0.0188 (14)	0.0001 (12)
C3	0.053 (2)	0.0348 (16)	0.0425 (18)	0.0100 (15)	0.0308 (17)	−0.0023 (14)
C4	0.058 (2)	0.0265 (14)	0.0301 (15)	0.0040 (13)	0.0265 (15)	−0.0015 (12)
C5	0.0466 (18)	0.0221 (13)	0.0253 (14)	−0.0029 (12)	0.0175 (14)	0.0012 (11)
C6	0.0359 (15)	0.0186 (12)	0.0233 (13)	−0.0018 (11)	0.0179 (12)	0.0015 (10)
C7	0.0316 (14)	0.0163 (11)	0.0248 (13)	−0.0002 (10)	0.0171 (12)	0.0015 (10)
O2	0.0241 (9)	0.0231 (9)	0.0205 (9)	0.0018 (7)	0.0114 (8)	−0.0003 (7)
C8	0.0269 (14)	0.0233 (13)	0.0187 (12)	−0.0019 (10)	0.0087 (11)	0.0029 (10)
N1	0.0223 (11)	0.0160 (10)	0.0195 (10)	0.0016 (8)	0.0084 (9)	0.0015 (8)
C9	0.0298 (14)	0.0190 (12)	0.0203 (13)	0.0059 (10)	0.0101 (11)	0.0059 (10)
C10	0.0316 (14)	0.0133 (11)	0.0267 (13)	0.0015 (10)	0.0162 (12)	0.0026 (10)
N2	0.0204 (10)	0.0165 (10)	0.0200 (10)	0.0006 (8)	0.0105 (9)	0.0011 (8)
C11	0.0239 (13)	0.0167 (12)	0.0300 (14)	−0.0032 (10)	0.0163 (11)	−0.0037 (10)
C12	0.0174 (12)	0.0229 (12)	0.0223 (12)	0.0001 (10)	0.0090 (10)	−0.0033 (10)
C13	0.0213 (13)	0.0258 (14)	0.0284 (14)	−0.0049 (11)	0.0093 (11)	−0.0083 (11)
C14	0.0223 (14)	0.0384 (16)	0.0220 (14)	−0.0031 (12)	0.0018 (12)	−0.0098 (12)
C15	0.0217 (13)	0.0381 (16)	0.0207 (13)	0.0050 (11)	0.0038 (11)	0.0010 (12)
C16	0.0210 (13)	0.0264 (13)	0.0204 (12)	0.0035 (10)	0.0081 (11)	0.0008 (10)
C17	0.0169 (12)	0.0242 (12)	0.0171 (11)	0.0016 (10)	0.0077 (10)	−0.0020 (10)
O3	0.0222 (9)	0.0182 (8)	0.0153 (8)	−0.0005 (7)	0.0058 (7)	−0.0007 (6)
O4	0.0324 (10)	0.0246 (9)	0.0189 (9)	0.0053 (8)	0.0050 (8)	0.0047 (7)
C18	0.0423 (17)	0.0325 (15)	0.0228 (14)	0.0113 (13)	0.0095 (13)	0.0095 (12)
C19	0.0300 (18)	0.088 (3)	0.078 (3)	0.0179 (18)	0.0030 (18)	−0.055 (2)
O5	0.0251 (10)	0.0362 (11)	0.0351 (11)	0.0055 (8)	0.0076 (9)	−0.0150 (9)
C20	0.0242 (13)	0.0273 (13)	0.0212 (13)	0.0014 (11)	0.0056 (11)	−0.0030 (10)
C21	0.0216 (14)	0.0390 (16)	0.0342 (16)	0.0070 (12)	0.0072 (13)	−0.0022 (13)
C22	0.0197 (14)	0.0407 (17)	0.0316 (15)	−0.0036 (12)	−0.0003 (12)	−0.0014 (13)
C23	0.0290 (15)	0.0260 (14)	0.0287 (14)	−0.0060 (12)	0.0040 (12)	−0.0041 (11)
C24	0.0231 (13)	0.0216 (12)	0.0205 (12)	−0.0018 (10)	0.0053 (11)	0.0003 (10)
C25	0.0222 (12)	0.0211 (12)	0.0141 (11)	−0.0013 (9)	0.0070 (10)	0.0011 (9)
O6	0.0181 (9)	0.0213 (8)	0.0178 (8)	−0.0005 (7)	0.0068 (7)	−0.0025 (7)
C26	0.0311 (15)	0.0167 (12)	0.0184 (12)	−0.0052 (10)	0.0077 (11)	−0.0021 (10)
N3	0.0247 (11)	0.0169 (10)	0.0135 (9)	0.0005 (8)	0.0072 (9)	0.0015 (8)
C27	0.0300 (15)	0.0155 (11)	0.0209 (13)	0.0024 (10)	0.0126 (12)	−0.0010 (10)
N4	0.074 (2)	0.060 (2)	0.087 (3)	0.0026 (19)	0.034 (2)	0.018 (2)
C28	0.080 (3)	0.059 (3)	0.097 (3)	0.022 (2)	0.052 (3)	0.021 (2)
C29	0.063 (3)	0.056 (2)	0.085 (3)	0.011 (2)	0.045 (2)	0.015 (2)
N5	0.077 (3)	0.054 (2)	0.157 (4)	−0.0058 (18)	0.078 (3)	−0.013 (2)
C30	0.058 (2)	0.0369 (17)	0.0483 (19)	−0.0017 (15)	0.0383 (17)	−0.0011 (14)
C31	0.055 (2)	0.0379 (18)	0.067 (2)	−0.0056 (16)	0.036 (2)	−0.0003 (16)

Geometric parameters (Å, º)

Co1—N1	1.8894 (19)	C14—H14	0.91 (3)
Co1—O3	1.8915 (16)	C15—C16	1.376 (4)
Co1—N2	1.9041 (19)	C15—H15	0.90 (3)
Co1—O2	1.9073 (17)	C16—O4	1.367 (3)
Co1—O6	1.9093 (16)	C16—C17	1.433 (3)
Co1—N3	1.9445 (19)	C17—O3	1.298 (3)
C1A—O1	1.395 (6)	O4—C18	1.431 (3)
C1A—H1AA	0.9800	C18—H18A	0.9800
C1A—H1AB	0.9800	C18—H18B	0.9800
C1A—H1AC	0.9800	C18—H18C	0.9800
C1B—O1	1.182 (8)	C19—O5	1.426 (3)
C1B—H1BA	0.9800	C19—H19A	0.9800
C1B—H1BB	0.9800	C19—H19B	0.9800
C1B—H1BC	0.9800	C19—H19C	0.9800
O1—C2	1.362 (4)	O5—C20	1.370 (3)
C2—C3	1.377 (4)	C20—C21	1.378 (4)
C2—C7	1.426 (4)	C20—C25	1.417 (3)
C3—C4	1.397 (4)	C21—C22	1.396 (4)
C3—H3	0.95 (4)	C21—H21	0.87 (3)
C4—C5	1.371 (4)	C22—C23	1.357 (4)
C4—H4	1.03 (3)	C22—H22	0.97 (3)
C5—C6	1.415 (4)	C23—C24	1.414 (4)
C5—H5	0.92 (3)	C23—H23	0.93 (3)
C6—C7	1.409 (4)	C24—C25	1.412 (3)
C6—C8	1.439 (3)	C24—C26	1.441 (3)
C7—O2	1.305 (3)	C25—O6	1.316 (3)
C8—N1	1.291 (3)	C26—N3	1.287 (3)
C8—H8	0.96 (3)	C26—H26	0.93 (3)
N1—C9	1.470 (3)	N3—C27	1.470 (3)
C9—C10	1.521 (4)	C27—C27^{i}	1.525 (5)
C9—H9A	0.95 (2)	C27—H27A	0.94 (2)
C9—H9B	0.99 (3)	C27—H27B	0.93 (3)
C10—N2	1.473 (3)	N4—C29	1.142 (5)
C10—H10A	0.95 (3)	C28—C29	1.466 (5)
C10—H10B	0.94 (3)	C28—H28A	0.9800
N2—C11	1.279 (3)	C28—H28B	0.9800
C11—C12	1.438 (3)	C28—H28C	0.9800
C11—H11	0.96 (2)	N5—C31	1.151 (4)
C12—C13	1.417 (3)	C30—C31	1.431 (5)
C12—C17	1.420 (3)	C30—H30A	0.9800
C13—C14	1.368 (4)	C30—H30B	0.9800
C13—H13	0.91 (3)	C30—H30C	0.9800
C14—C15	1.396 (4)		
N1—Co1—O3	175.48 (8)	C14—C13—C12	120.6 (2)
N1—Co1—N2	83.12 (8)	C14—C13—H13	115.8 (17)

O3—Co1—N2	95.06 (8)	C12—C13—H13	123.6 (17)
N1—Co1—O2	88.53 (8)	C13—C14—C15	119.9 (2)
O3—Co1—O2	87.40 (7)	C13—C14—H14	120.0 (17)
N2—Co1—O2	92.16 (8)	C15—C14—H14	120.0 (17)
N1—Co1—O6	92.38 (8)	C16—C15—C14	121.0 (3)
O3—Co1—O6	91.57 (7)	C16—C15—H15	119.3 (17)
N2—Co1—O6	84.89 (8)	C14—C15—H15	119.7 (17)
O2—Co1—O6	176.78 (7)	O4—C16—C15	125.1 (2)
N1—Co1—N3	94.20 (8)	O4—C16—C17	113.9 (2)
O3—Co1—N3	87.99 (7)	C15—C16—C17	121.0 (2)
N2—Co1—N3	174.09 (8)	O3—C17—C12	125.7 (2)
O2—Co1—N3	93.04 (8)	O3—C17—C16	117.4 (2)
O6—Co1—N3	89.97 (8)	C12—C17—C16	116.9 (2)
O1—C1A—H1AA	109.5	C17—O3—Co1	125.75 (15)
O1—C1A—H1AB	109.5	C16—O4—C18	117.1 (2)
H1AA—C1A—H1AB	109.5	O4—C18—H18A	109.5
O1—C1A—H1AC	109.5	O4—C18—H18B	109.5
H1AA—C1A—H1AC	109.5	H18A—C18—H18B	109.5
H1AB—C1A—H1AC	109.5	O4—C18—H18C	109.5
O1—C1B—H1BA	109.5	H18A—C18—H18C	109.5
O1—C1B—H1BB	109.5	H18B—C18—H18C	109.5
H1BA—C1B—H1BB	109.5	O5—C19—H19A	109.5
O1—C1B—H1BC	109.5	O5—C19—H19B	109.5
H1BA—C1B—H1BC	109.5	H19A—C19—H19B	109.5
H1BB—C1B—H1BC	109.5	O5—C19—H19C	109.5
C1B—O1—C2	123.7 (5)	H19A—C19—H19C	109.5
C2—O1—C1A	121.4 (3)	H19B—C19—H19C	109.5
O1—C2—C3	122.5 (3)	C20—O5—C19	117.7 (2)
O1—C2—C7	116.6 (2)	O5—C20—C21	124.5 (2)
C3—C2—C7	120.9 (3)	O5—C20—C25	114.5 (2)
C2—C3—C4	120.6 (3)	C21—C20—C25	121.0 (2)
C2—C3—H3	120 (2)	C20—C21—C22	120.9 (3)
C4—C3—H3	119 (2)	C20—C21—H21	121 (2)
C5—C4—C3	120.1 (3)	C22—C21—H21	118 (2)
C5—C4—H4	122.4 (18)	C23—C22—C21	119.8 (3)
C3—C4—H4	117.4 (17)	C23—C22—H22	121.4 (18)
C4—C5—C6	120.1 (3)	C21—C22—H22	118.7 (18)
C4—C5—H5	124.6 (17)	C22—C23—C24	120.7 (3)
C6—C5—H5	115.3 (17)	C22—C23—H23	122.3 (19)
C7—C6—C5	120.7 (2)	C24—C23—H23	116.9 (19)
C7—C6—C8	117.5 (2)	C25—C24—C23	120.5 (2)
C5—C6—C8	120.0 (2)	C25—C24—C26	119.9 (2)
O2—C7—C6	124.7 (2)	C23—C24—C26	119.0 (2)
O2—C7—C2	117.8 (2)	O6—C25—C24	124.1 (2)
C6—C7—C2	117.3 (2)	O6—C25—C20	118.6 (2)
C7—O2—Co1	121.35 (16)	C24—C25—C20	117.2 (2)
N1—C8—C6	123.3 (2)	C25—O6—Co1	121.60 (14)
N1—C8—H8	118.6 (16)	N3—C26—C24	125.8 (2)

C6—C8—H8	117.4 (16)	N3—C26—H26	119.4 (15)
C8—N1—C9	119.9 (2)	C24—C26—H26	114.6 (15)
C8—N1—Co1	125.26 (17)	C26—N3—C27	115.8 (2)
C9—N1—Co1	111.06 (15)	C26—N3—Co1	122.42 (17)
N1—C9—C10	102.7 (2)	C27—N3—Co1	121.63 (16)
N1—C9—H9A	111.9 (14)	N3—C27—C27^{i}	109.7 (2)
C10—C9—H9A	109.5 (14)	N3—C27—H27A	109.7 (15)
N1—C9—H9B	111.7 (15)	C27^{i}—C27—H27A	110.1 (15)
C10—C9—H9B	111.5 (15)	N3—C27—H27B	110.4 (15)
H9A—C9—H9B	109 (2)	C27^{i}—C27—H27B	109.6 (15)
N2—C10—C9	107.97 (19)	H27A—C27—H27B	107 (2)
N2—C10—H10A	107.6 (15)	C29—C28—H28A	109.5
C9—C10—H10A	111.0 (15)	C29—C28—H28B	109.5
N2—C10—H10B	110.5 (17)	H28A—C28—H28B	109.5
C9—C10—H10B	110.1 (17)	C29—C28—H28C	109.5
H10A—C10—H10B	110 (2)	H28A—C28—H28C	109.5
C11—N2—C10	120.5 (2)	H28B—C28—H28C	109.5
C11—N2—Co1	125.72 (17)	N4—C29—C28	179.6 (6)
C10—N2—Co1	113.68 (15)	C31—C30—H30A	109.5
N2—C11—C12	125.8 (2)	C31—C30—H30B	109.5
N2—C11—H11	119.5 (15)	H30A—C30—H30B	109.5
C12—C11—H11	114.8 (15)	C31—C30—H30C	109.5
C13—C12—C17	120.4 (2)	H30A—C30—H30C	109.5
C13—C12—C11	117.7 (2)	H30B—C30—H30C	109.5
C17—C12—C11	121.9 (2)	N5—C31—C30	176.3 (4)

C1B—O1—C2—C3	105.3 (6)	C13—C14—C15—C16	2.2 (4)
C1A—O1—C2—C3	15.2 (6)	C14—C15—C16—O4	179.3 (2)
C1B—O1—C2—C7	−75.6 (6)	C14—C15—C16—C17	−0.3 (4)
C1A—O1—C2—C7	−165.6 (4)	C13—C12—C17—O3	−176.4 (2)
O1—C2—C3—C4	−178.9 (3)	C11—C12—C17—O3	2.9 (4)
C7—C2—C3—C4	2.1 (5)	C13—C12—C17—C16	4.1 (3)
C2—C3—C4—C5	−3.4 (5)	C11—C12—C17—C16	−176.6 (2)
C3—C4—C5—C6	0.8 (4)	O4—C16—C17—O3	−2.0 (3)
C4—C5—C6—C7	3.2 (4)	C15—C16—C17—O3	177.7 (2)
C4—C5—C6—C8	−161.2 (3)	O4—C16—C17—C12	177.6 (2)
C5—C6—C7—O2	179.3 (2)	C15—C16—C17—C12	−2.7 (4)
C8—C6—C7—O2	−15.9 (4)	C12—C17—O3—Co1	−4.1 (3)
C5—C6—C7—C2	−4.5 (4)	C16—C17—O3—Co1	175.44 (16)
C8—C6—C7—C2	160.3 (2)	N2—Co1—O3—C17	1.57 (19)
O1—C2—C7—O2	−0.8 (4)	O2—Co1—O3—C17	−90.37 (18)
C3—C2—C7—O2	178.4 (3)	O6—Co1—O3—C17	86.58 (18)
O1—C2—C7—C6	−177.3 (3)	N3—Co1—O3—C17	176.50 (19)
C3—C2—C7—C6	1.9 (4)	C15—C16—O4—C18	10.9 (4)
C6—C7—O2—Co1	−25.3 (3)	C17—C16—O4—C18	−169.5 (2)
C2—C7—O2—Co1	158.48 (18)	C19—O5—C20—C21	−7.2 (4)
C7—C6—C8—N1	27.2 (4)	C19—O5—C20—C25	172.4 (3)
C5—C6—C8—N1	−167.9 (2)	O5—C20—C21—C22	179.6 (3)

C6—C8—N1—C9	−151.1 (2)	C25—C20—C21—C22	0.0 (4)
C6—C8—N1—Co1	5.1 (4)	C20—C21—C22—C23	−0.9 (5)
N2—Co1—N1—C8	−125.7 (2)	C21—C22—C23—C24	1.2 (4)
O2—Co1—N1—C8	−33.4 (2)	C22—C23—C24—C25	−0.7 (4)
O6—Co1—N1—C8	149.7 (2)	C22—C23—C24—C26	−171.9 (3)
N3—Co1—N1—C8	59.6 (2)	C23—C24—C25—O6	−177.7 (2)
N2—Co1—N1—C9	32.29 (16)	C26—C24—C25—O6	−6.6 (4)
O2—Co1—N1—C9	124.64 (17)	C23—C24—C25—C20	−0.1 (4)
O6—Co1—N1—C9	−52.28 (17)	C26—C24—C25—C20	171.0 (2)
N3—Co1—N1—C9	−142.42 (17)	O5—C20—C25—O6	−1.5 (3)
C8—N1—C9—C10	110.2 (3)	C21—C20—C25—O6	178.2 (2)
Co1—N1—C9—C10	−49.1 (2)	O5—C20—C25—C24	−179.2 (2)
N1—C9—C10—N2	42.5 (3)	C21—C20—C25—C24	0.4 (4)
C9—C10—N2—C11	156.2 (2)	C24—C25—O6—Co1	−29.1 (3)
C9—C10—N2—Co1	−20.2 (2)	C20—C25—O6—Co1	153.33 (18)
C10—N2—C11—C12	−179.6 (2)	C25—C24—C26—N3	16.9 (4)
Co1—N2—C11—C12	−3.7 (4)	C23—C24—C26—N3	−171.9 (2)
N2—C11—C12—C13	−179.3 (2)	C24—C26—N3—C27	−166.0 (2)
N2—C11—C12—C17	1.3 (4)	C24—C26—N3—Co1	10.1 (3)
C17—C12—C13—C14	−2.4 (4)	C26—N3—C27—C27^{i}	74.9 (3)
C11—C12—C13—C14	178.3 (2)	Co1—N3—C27—C27^{i}	−101.3 (3)
C12—C13—C14—C15	−0.8 (4)		

Symmetry code: (i) −*x*+1, −*y*+1, −*z*+1.

Hydrogen-bond geometry (Å, º)

D—H···*A*	*D*—H	H···*A*	*D*···*A*	*D*—H···*A*
C1*B*—H1*BA*···N4^{ii}	0.98	2.59	3.333 (10)	133
C1*B*—H1*BB*···O2	0.98	2.44	2.985 (8)	115
C8—H8···O5^{iii}	0.96 (3)	2.34 (3)	3.119 (3)	138 (2)
C9—H9*B*···O6	1.00 (3)	2.51 (2)	2.924 (3)	104.6 (17)
C27—H27*A*···O2	0.94 (2)	2.45 (2)	3.042 (3)	121.1 (18)
C27—H27*B*···O3^{i}	0.93 (3)	2.53 (2)	3.180 (3)	127.5 (18)
C28—H28*C*···O1^{iv}	0.98	2.52	3.266 (5)	133
C30—H30*C*···O3	0.98	2.52	3.188 (3)	126
C30—H30*C*···O6	0.98	2.34	3.245 (3)	153
C9—H9*A*···O5^{iii}	0.95 (2)	2.64 (2)	3.293 (3)	126.8 (18)

Symmetry codes: (i) −*x*+1, −*y*+1, −*z*+1; (ii) *x*−1, *y*, *z*; (iii) *x*, −*y*+1/2, *z*+1/2; (iv) *x*+1, *y*, *z*.

{*μ*-6,6′-Dimethoxy-2,2′-[ethane-1,2-diylbis(nitrilomethylylidene)]diphenolato}bis({6,6′-dimethoxy-2,2′-[ethane-1,2-diylbis(nitrilomethylylidene)]diphenolato}cobalt(III)) acetonitrile tetrasolvate (3)

Crystal data

$[Co_2(C_{18}H_{18}N_2O_4)_3]\cdot 4C_2H_3N$
M_r = 1261.10
Triclinic, $P\overline{1}$
a = 10.4971 (5) Å
b = 11.6195 (5) Å
c = 13.7158 (6) Å
α = 70.471 (4)°
β = 71.667 (4)°
γ = 72.466 (4)°
V = 1460.26 (13) Å^3

$Z = 1$
$F(000) = 658$
$D_x = 1.434$ Mg m^{-3}
Mo $K\alpha$ radiation, $\lambda = 0.71073$ Å
Cell parameters from 9604 reflections
$\theta = 3.5$–$29.7°$
$\mu = 0.64$ mm^{-1}
$T = 100$ K
Block, black
0.21 × 0.14 × 0.05 mm

Data collection

Rigaku Xcalibur Sapphire3 diffractometer
Radiation source: fine-focus sealed X-ray tube, Enhance (Mo) X-ray Source
Detector resolution: 16.0655 pixels mm^{-1}
ω scans
Absorption correction: multi-scan (CrysAlis PRO; Rigaku OD, 2015)
$T_{min} = 0.835$, $T_{max} = 1.000$
20710 measured reflections
6041 independent reflections
5192 reflections with $I > 2\sigma(I)$
$R_{int} = 0.039$
$\theta_{max} = 26.5°$, $\theta_{min} = 3.3°$
$h = -13 \rightarrow 13$
$k = -14 \rightarrow 14$
$l = -17 \rightarrow 17$

Refinement

Refinement on F^2
Least-squares matrix: full
$R[F^2 > 2\sigma(F^2)] = 0.037$
$wR(F^2) = 0.094$
$S = 1.04$
6041 reflections
421 parameters
3 restraints
Primary atom site location: iterative
Hydrogen site location: mixed
H atoms treated by a mixture of independent and constrained refinement
$w = 1/[\sigma^2(F_o^2) + (0.0446P)^2 + 0.822P]$ where $P = (F_o^2 + 2F_c^2)/3$
$(\Delta/\sigma)_{max} = 0.001$
$\Delta\rho_{max} = 0.89$ e Å^{-3}
$\Delta\rho_{min} = -0.35$ e Å^{-3}

Special details

Geometry. All esds (except the esd in the dihedral angle between two l.s. planes) are estimated using the full covariance matrix. The cell esds are taken into account individually in the estimation of esds in distances, angles and torsion angles; correlations between esds in cell parameters are only used when they are defined by crystal symmetry. An approximate (isotropic) treatment of cell esds is used for estimating esds involving l.s. planes.

Fractional atomic coordinates and isotropic or equivalent isotropic displacement parameters (Å²)

	x	*y*	*z*	U_{iso}*/U_{eq}	Occ. (<1)
Co1	0.63637 (3)	0.21886 (2)	0.45402 (2)	0.01484 (9)	
O1	0.23568 (15)	0.26331 (15)	0.67591 (12)	0.0293 (4)	
O2	0.47661 (13)	0.18304 (12)	0.56136 (10)	0.0185 (3)	
O3	0.51922 (13)	0.33725 (12)	0.36826 (10)	0.0177 (3)	
O4	0.37763 (14)	0.53359 (12)	0.25864 (11)	0.0219 (3)	
N1	0.74411 (16)	0.09203 (14)	0.54317 (13)	0.0171 (3)	
N2	0.65403 (16)	0.08537 (14)	0.39518 (13)	0.0172 (3)	
C1	0.1079 (2)	0.3228 (3)	0.7331 (2)	0.0426 (6)	
H1A	0.041470	0.356060	0.688396	0.064*	
H1B	0.072734	0.261729	0.798001	0.064*	
H1C	0.121711	0.391431	0.752317	0.064*	
C2	0.3402 (2)	0.21155 (19)	0.72749 (17)	0.0241 (4)	
C3	0.3262 (2)	0.1959 (2)	0.83433 (17)	0.0289 (5)	
H3	0.238339	0.222060	0.877606	0.035*	
C4	0.4406 (3)	0.1416 (2)	0.88001 (17)	0.0309 (5)	

H4	0.429773	0.131728	0.953581	0.037*
C5	0.5673 (2)	0.10318 (19)	0.81838 (17)	0.0277 (5)
H5	0.644158	0.065761	0.849459	0.033*
C6	0.5844 (2)	0.11892 (18)	0.70842 (16)	0.0210 (4)
C7	0.4708 (2)	0.17191 (17)	0.66052 (15)	0.0193 (4)
C8	0.7120 (2)	0.06237 (18)	0.64607 (16)	0.0214 (4)
H8	0.773 (2)	−0.005 (2)	0.6828 (17)	0.019 (5)*
C9	0.8363 (2)	−0.00101 (18)	0.48614 (16)	0.0198 (4)
H9A	0.881765	−0.074872	0.534752	0.024*
H9B	0.907275	0.035716	0.426634	0.024*
C10	0.7366 (2)	−0.03519 (18)	0.44532 (17)	0.0210 (4)
H10A	0.787483	−0.084173	0.392654	0.025*
H10B	0.676687	−0.085254	0.504838	0.025*
C11	0.6162 (2)	0.09788 (19)	0.31161 (16)	0.0197 (4)
H11	0.637 (2)	0.030 (2)	0.2869 (18)	0.024 (6)*
C12	0.5445 (2)	0.21185 (18)	0.25094 (16)	0.0190 (4)
C13	0.5236 (2)	0.2110 (2)	0.15418 (16)	0.0230 (4)
H13	0.554402	0.135458	0.132768	0.028*
C14	0.4603 (2)	0.3164 (2)	0.09127 (16)	0.0245 (4)
H14	0.450262	0.315110	0.025204	0.029*
C15	0.4096 (2)	0.42734 (19)	0.12433 (16)	0.0214 (4)
H15	0.363781	0.500511	0.081051	0.026*
C16	0.42598 (19)	0.43068 (18)	0.21882 (15)	0.0178 (4)
C17	0.50010 (18)	0.32394 (18)	0.28402 (15)	0.0160 (4)
C18	0.2875 (2)	0.6376 (2)	0.20569 (18)	0.0279 (5)
H18A	0.259958	0.704980	0.241049	0.042*
H18B	0.335034	0.667728	0.131224	0.042*
H18C	0.205603	0.611556	0.208484	0.042*
O5	1.03652 (14)	0.22470 (14)	0.21059 (11)	0.0244 (3)
O6	0.79600 (13)	0.25601 (12)	0.34514 (10)	0.0167 (3)
N3	0.63436 (16)	0.35219 (14)	0.50880 (12)	0.0157 (3)
C19	1.1576 (2)	0.2330 (2)	0.12618 (17)	0.0271 (5)
H19A	1.152160	0.200627	0.070493	0.041*
H19B	1.165163	0.320617	0.096228	0.041*
H19C	1.238555	0.183406	0.153889	0.041*
C20	1.0295 (2)	0.26700 (17)	0.29500 (15)	0.0186 (4)
C21	1.1393 (2)	0.29228 (18)	0.31310 (16)	0.0210 (4)
H21	1.227025	0.280547	0.265120	0.025*
C22	1.1227 (2)	0.33502 (18)	0.40145 (16)	0.0221 (4)
H22	1.199343	0.349469	0.414712	0.027*
C23	0.9953 (2)	0.35583 (18)	0.46853 (16)	0.0212 (4)
H23	0.983456	0.387243	0.527215	0.025*
C24	0.88111 (19)	0.33113 (17)	0.45152 (15)	0.0173 (4)
C25	0.89633 (19)	0.28245 (16)	0.36588 (15)	0.0162 (4)
C26	0.7448 (2)	0.37803 (18)	0.50954 (15)	0.0178 (4)
H26	0.733 (2)	0.442 (2)	0.5422 (17)	0.017 (5)*
C27	0.50441 (19)	0.43761 (16)	0.54340 (15)	0.0172 (4)
H27A	0.501559	0.451444	0.611539	0.021*

H27B	0.425588	0.400949	0.554346	0.021*	
N4	0.9291 (3)	0.3870 (3)	−0.0371 (2)	0.0653 (8)	
C29	0.8603 (3)	0.4235 (3)	0.0334 (2)	0.0400 (6)	
C28	0.7738 (3)	0.4709 (2)	0.12272 (19)	0.0389 (6)	
H28A	0.770618	0.402227	0.188075	0.047*	
H28B	0.680675	0.507736	0.111576	0.047*	
H28C	0.811328	0.534972	0.129214	0.047*	
C30	0.8972 (3)	0.0892 (4)	0.1166 (3)	0.0754 (11)	
H30A	0.827835	0.052200	0.111382	0.113*	0.43 (2)
H30B	0.943101	0.131554	0.045009	0.113*	0.43 (2)
H30C	0.852468	0.149867	0.159040	0.113*	0.43 (2)
H30D	0.908195	0.159725	0.053059	0.113*	0.57 (2)
H30E	0.867133	0.119634	0.180507	0.113*	0.57 (2)
H30F	0.828092	0.048893	0.115509	0.113*	0.57 (2)
C31B	1.0279 (10)	−0.0010 (8)	0.1174 (11)	0.054 (3)	0.57 (2)
N5B	1.1381 (15)	−0.0601 (11)	0.1001 (19)	0.140 (8)	0.57 (2)
C31A	0.9957 (14)	−0.0065 (12)	0.1661 (14)	0.070 (5)	0.43 (2)
N5A	1.0772 (12)	−0.0821 (8)	0.2000 (19)	0.106 (6)	0.43 (2)

Atomic displacement parameters (Å²)

	U^{11}	U^{22}	U^{33}	U^{12}	U^{13}	U^{23}
Co1	0.01524 (14)	0.01267 (13)	0.01716 (14)	−0.00227 (10)	−0.00561 (10)	−0.00369 (10)
O1	0.0200 (8)	0.0428 (9)	0.0286 (8)	−0.0042 (7)	−0.0022 (6)	−0.0194 (7)
O2	0.0192 (7)	0.0193 (7)	0.0187 (7)	−0.0067 (6)	−0.0036 (5)	−0.0057 (6)
O3	0.0190 (7)	0.0165 (6)	0.0195 (7)	−0.0011 (5)	−0.0086 (5)	−0.0056 (5)
O4	0.0237 (7)	0.0174 (7)	0.0251 (7)	0.0010 (6)	−0.0125 (6)	−0.0049 (6)
N1	0.0170 (8)	0.0142 (8)	0.0217 (8)	−0.0042 (6)	−0.0062 (7)	−0.0044 (7)
N2	0.0139 (8)	0.0148 (8)	0.0226 (9)	−0.0024 (6)	−0.0043 (6)	−0.0051 (7)
C1	0.0263 (13)	0.0625 (18)	0.0375 (14)	0.0020 (12)	−0.0031 (10)	−0.0258 (13)
C2	0.0261 (11)	0.0232 (10)	0.0252 (11)	−0.0091 (9)	−0.0028 (9)	−0.0089 (9)
C3	0.0323 (12)	0.0278 (11)	0.0248 (11)	−0.0083 (9)	0.0012 (9)	−0.0105 (9)
C4	0.0479 (14)	0.0265 (11)	0.0165 (10)	−0.0083 (10)	−0.0044 (10)	−0.0064 (9)
C5	0.0384 (13)	0.0207 (10)	0.0236 (11)	−0.0059 (9)	−0.0107 (9)	−0.0028 (9)
C6	0.0282 (11)	0.0145 (9)	0.0196 (10)	−0.0075 (8)	−0.0052 (8)	−0.0014 (8)
C7	0.0239 (10)	0.0153 (9)	0.0203 (10)	−0.0093 (8)	−0.0021 (8)	−0.0051 (8)
C8	0.0269 (11)	0.0144 (9)	0.0239 (11)	−0.0051 (8)	−0.0116 (9)	−0.0007 (8)
C9	0.0192 (10)	0.0145 (9)	0.0245 (10)	0.0004 (8)	−0.0077 (8)	−0.0051 (8)
C10	0.0228 (10)	0.0134 (9)	0.0274 (11)	−0.0014 (8)	−0.0088 (8)	−0.0057 (8)
C11	0.0189 (10)	0.0183 (10)	0.0242 (10)	−0.0038 (8)	−0.0037 (8)	−0.0103 (8)
C12	0.0166 (10)	0.0212 (10)	0.0211 (10)	−0.0055 (8)	−0.0040 (8)	−0.0071 (8)
C13	0.0215 (10)	0.0279 (11)	0.0232 (10)	−0.0059 (9)	−0.0033 (8)	−0.0125 (9)
C14	0.0235 (11)	0.0366 (12)	0.0174 (10)	−0.0096 (9)	−0.0051 (8)	−0.0092 (9)
C15	0.0180 (10)	0.0256 (10)	0.0189 (10)	−0.0065 (8)	−0.0064 (8)	−0.0003 (8)
C16	0.0134 (9)	0.0200 (10)	0.0211 (10)	−0.0057 (7)	−0.0040 (7)	−0.0049 (8)
C17	0.0117 (9)	0.0200 (9)	0.0171 (9)	−0.0055 (7)	−0.0025 (7)	−0.0048 (8)
C18	0.0284 (12)	0.0217 (11)	0.0292 (12)	0.0035 (9)	−0.0134 (9)	−0.0030 (9)
O5	0.0197 (7)	0.0341 (8)	0.0217 (7)	−0.0087 (6)	0.0005 (6)	−0.0130 (6)

O6	0.0166 (7)	0.0170 (6)	0.0188 (7)	−0.0044 (5)	−0.0066 (5)	−0.0049 (5)
N3	0.0170 (8)	0.0131 (7)	0.0158 (8)	−0.0014 (6)	−0.0051 (6)	−0.0030 (6)
C19	0.0210 (11)	0.0358 (12)	0.0212 (11)	−0.0050 (9)	−0.0003 (8)	−0.0087 (9)
C20	0.0200 (10)	0.0159 (9)	0.0193 (10)	−0.0032 (8)	−0.0051 (8)	−0.0040 (8)
C21	0.0169 (10)	0.0179 (9)	0.0250 (10)	−0.0047 (8)	−0.0033 (8)	−0.0025 (8)
C22	0.0203 (10)	0.0197 (10)	0.0289 (11)	−0.0068 (8)	−0.0098 (8)	−0.0038 (8)
C23	0.0262 (11)	0.0183 (10)	0.0223 (10)	−0.0071 (8)	−0.0087 (8)	−0.0047 (8)
C24	0.0183 (10)	0.0133 (9)	0.0199 (10)	−0.0032 (7)	−0.0061 (8)	−0.0025 (7)
C25	0.0177 (9)	0.0109 (8)	0.0186 (9)	−0.0024 (7)	−0.0073 (7)	0.0001 (7)
C26	0.0239 (10)	0.0147 (9)	0.0155 (9)	−0.0049 (8)	−0.0049 (8)	−0.0041 (8)
C27	0.0179 (10)	0.0139 (9)	0.0192 (10)	−0.0025 (7)	−0.0040 (8)	−0.0050 (8)
N4	0.0631 (18)	0.087 (2)	0.0395 (14)	−0.0023 (15)	−0.0144 (13)	−0.0200 (14)
C29	0.0344 (14)	0.0509 (16)	0.0328 (14)	−0.0088 (12)	−0.0163 (11)	−0.0012 (12)
C28	0.0349 (14)	0.0427 (14)	0.0321 (13)	−0.0115 (11)	−0.0094 (11)	0.0027 (11)
C30	0.0428 (19)	0.098 (3)	0.098 (3)	−0.0213 (19)	0.0023 (19)	−0.054 (2)
C31B	0.063 (6)	0.037 (4)	0.075 (7)	−0.015 (4)	−0.041 (5)	−0.003 (4)
N5B	0.123 (9)	0.077 (5)	0.28 (2)	0.030 (6)	−0.142 (12)	−0.075 (9)
C31A	0.065 (7)	0.055 (8)	0.095 (10)	−0.027 (6)	0.006 (8)	−0.038 (8)
N5A	0.065 (6)	0.030 (4)	0.216 (18)	0.012 (4)	−0.055 (9)	−0.024 (6)

Geometric parameters (Å, º)

Co1—O3	1.8966 (13)	C15—C16	1.374 (3)
Co1—N1	1.8993 (16)	C15—H15	0.9500
Co1—O2	1.9002 (13)	C16—C17	1.435 (3)
Co1—O6	1.9118 (13)	C18—H18A	0.9800
Co1—N2	1.9133 (16)	C18—H18B	0.9800
Co1—N3	1.9271 (16)	C18—H18C	0.9800
O1—C2	1.368 (3)	O5—C20	1.376 (2)
O1—C1	1.426 (3)	O5—C19	1.428 (2)
O2—C7	1.306 (2)	O6—C25	1.314 (2)
O3—C17	1.297 (2)	N3—C26	1.286 (3)
O4—C16	1.372 (2)	N3—C27	1.471 (2)
O4—C18	1.428 (2)	C19—H19A	0.9800
N1—C8	1.292 (3)	C19—H19B	0.9800
N1—C9	1.475 (2)	C19—H19C	0.9800
N2—C11	1.278 (3)	C20—C21	1.382 (3)
N2—C10	1.478 (2)	C20—C25	1.429 (3)
C1—H1A	0.9800	C21—C22	1.401 (3)
C1—H1B	0.9800	C21—H21	0.9500
C1—H1C	0.9800	C22—C23	1.368 (3)
C2—C3	1.380 (3)	C22—H22	0.9500
C2—C7	1.430 (3)	C23—C24	1.415 (3)
C3—C4	1.409 (3)	C23—H23	0.9500
C3—H3	0.9500	C24—C25	1.413 (3)
C4—C5	1.367 (3)	C24—C26	1.443 (3)
C4—H4	0.9500	C26—H26	0.95 (2)
C5—C6	1.416 (3)	C27—C27^{i}	1.537 (4)

C5—H5	0.9500	C27—H27A	0.9900
C6—C7	1.419 (3)	C27—H27B	0.9900
C6—C8	1.443 (3)	N4—C29	1.135 (3)
C8—H8	0.95 (2)	C29—C28	1.441 (4)
C9—C10	1.528 (3)	C28—H28A	0.9800
C9—H9A	0.9900	C28—H28B	0.9800
C9—H9B	0.9900	C28—H28C	0.9800
C10—H10A	0.9900	C30—C31A	1.419 (12)
C10—H10B	0.9900	C30—C31B	1.455 (9)
C11—C12	1.438 (3)	C30—H30A	0.9800
C11—H11	0.90 (2)	C30—H30B	0.9800
C12—C13	1.415 (3)	C30—H30C	0.9800
C12—C17	1.420 (3)	C30—H30D	0.9800
C13—C14	1.361 (3)	C30—H30E	0.9800
C13—H13	0.9500	C30—H30F	0.9800
C14—C15	1.405 (3)	C31B—N5B	1.150 (9)
C14—H14	0.9500	C31A—N5A	1.115 (11)

O3—Co1—N1	175.58 (6)	C15—C14—H14	120.1
O3—Co1—O2	88.27 (6)	C16—C15—C14	120.45 (19)
N1—Co1—O2	88.36 (6)	C16—C15—H15	119.8
O3—Co1—O6	91.18 (6)	C14—C15—H15	119.8
N1—Co1—O6	92.19 (6)	O4—C16—C15	124.60 (18)
O2—Co1—O6	179.45 (6)	O4—C16—C17	113.90 (17)
O3—Co1—N2	94.41 (6)	C15—C16—C17	121.48 (18)
N1—Co1—N2	82.96 (7)	O3—C17—C12	125.71 (18)
O2—Co1—N2	93.67 (6)	O3—C17—C16	117.71 (17)
O6—Co1—N2	86.35 (6)	C12—C17—C16	116.58 (18)
O3—Co1—N3	87.74 (6)	O4—C18—H18A	109.5
N1—Co1—N3	95.15 (7)	O4—C18—H18B	109.5
O2—Co1—N3	90.49 (6)	H18A—C18—H18B	109.5
O6—Co1—N3	89.51 (6)	O4—C18—H18C	109.5
N2—Co1—N3	175.37 (7)	H18A—C18—H18C	109.5
C2—O1—C1	116.89 (17)	H18B—C18—H18C	109.5
C7—O2—Co1	119.80 (12)	C20—O5—C19	116.09 (16)
C17—O3—Co1	125.19 (12)	C25—O6—Co1	121.37 (12)
C16—O4—C18	116.92 (16)	C26—N3—C27	116.22 (16)
C8—N1—C9	120.10 (16)	C26—N3—Co1	122.79 (13)
C8—N1—Co1	125.38 (14)	C27—N3—Co1	120.76 (12)
C9—N1—Co1	110.26 (12)	O5—C19—H19A	109.5
C11—N2—C10	120.50 (17)	O5—C19—H19B	109.5
C11—N2—Co1	125.18 (14)	H19A—C19—H19B	109.5
C10—N2—Co1	113.70 (13)	O5—C19—H19C	109.5
O1—C1—H1A	109.5	H19A—C19—H19C	109.5
O1—C1—H1B	109.5	H19B—C19—H19C	109.5
H1A—C1—H1B	109.5	O5—C20—C21	124.61 (18)
O1—C1—H1C	109.5	O5—C20—C25	114.11 (17)
H1A—C1—H1C	109.5	C21—C20—C25	121.28 (18)

H1B—C1—H1C	109.5	C20—C21—C22	120.71 (18)
O1—C2—C3	125.13 (19)	C20—C21—H21	119.6
O1—C2—C7	113.95 (18)	C22—C21—H21	119.6
C3—C2—C7	120.9 (2)	C23—C22—C21	119.58 (19)
C2—C3—C4	120.8 (2)	C23—C22—H22	120.2
C2—C3—H3	119.6	C21—C22—H22	120.2
C4—C3—H3	119.6	C22—C23—C24	120.79 (19)
C5—C4—C3	120.0 (2)	C22—C23—H23	119.6
C5—C4—H4	120.0	C24—C23—H23	119.6
C3—C4—H4	120.0	C25—C24—C23	120.78 (18)
C4—C5—C6	120.3 (2)	C25—C24—C26	119.29 (18)
C4—C5—H5	119.9	C23—C24—C26	118.89 (18)
C6—C5—H5	119.9	O6—C25—C24	124.57 (17)
C5—C6—C7	121.01 (19)	O6—C25—C20	118.62 (17)
C5—C6—C8	120.71 (19)	C24—C25—C20	116.74 (17)
C7—C6—C8	117.44 (18)	N3—C26—C24	124.80 (18)
O2—C7—C6	124.69 (18)	N3—C26—H26	116.6 (13)
O2—C7—C2	118.25 (18)	C24—C26—H26	117.9 (13)
C6—C7—C2	117.02 (18)	N3—C27—C27^{i}	108.27 (18)
N1—C8—C6	123.55 (18)	N3—C27—H27A	110.0
N1—C8—H8	118.1 (13)	C27^{i}—C27—H27A	110.0
C6—C8—H8	118.1 (13)	N3—C27—H27B	110.0
N1—C9—C10	102.13 (15)	C27^{i}—C27—H27B	110.0
N1—C9—H9A	111.3	H27A—C27—H27B	108.4
C10—C9—H9A	111.3	N4—C29—C28	179.3 (3)
N1—C9—H9B	111.3	C29—C28—H28A	109.5
C10—C9—H9B	111.3	C29—C28—H28B	109.5
H9A—C9—H9B	109.2	H28A—C28—H28B	109.5
N2—C10—C9	105.55 (15)	C29—C28—H28C	109.5
N2—C10—H10A	110.6	H28A—C28—H28C	109.5
C9—C10—H10A	110.6	H28B—C28—H28C	109.5
N2—C10—H10B	110.6	C31A—C30—H30A	109.5
C9—C10—H10B	110.6	C31A—C30—H30B	109.5
H10A—C10—H10B	108.8	H30A—C30—H30B	109.5
N2—C11—C12	126.03 (19)	C31A—C30—H30C	109.5
N2—C11—H11	118.0 (15)	H30A—C30—H30C	109.5
C12—C11—H11	115.9 (15)	H30B—C30—H30C	109.5
C13—C12—C17	120.31 (19)	C31B—C30—H30D	109.5
C13—C12—C11	118.06 (18)	C31B—C30—H30E	109.5
C17—C12—C11	121.58 (19)	H30D—C30—H30E	109.5
C14—C13—C12	121.15 (19)	C31B—C30—H30F	109.5
C14—C13—H13	119.4	H30D—C30—H30F	109.5
C12—C13—H13	119.4	H30E—C30—H30F	109.5
C13—C14—C15	119.8 (2)	N5B—C31B—C30	168.0 (12)
C13—C14—H14	120.1	N5A—C31A—C30	176.4 (16)
O2—Co1—O3—C17	−108.49 (15)	C17—C12—C13—C14	−0.4 (3)
O6—Co1—O3—C17	71.50 (15)	C11—C12—C13—C14	−178.03 (18)

N2—Co1—O3—C17	−14.94 (15)	C12—C13—C14—C15	−2.5 (3)
N3—Co1—O3—C17	160.96 (15)	C13—C14—C15—C16	1.2 (3)
O2—Co1—N1—C8	−32.07 (17)	C18—O4—C16—C15	9.5 (3)
O6—Co1—N1—C8	147.98 (16)	C18—O4—C16—C17	−171.85 (16)
N2—Co1—N1—C8	−125.97 (17)	C14—C15—C16—O4	−178.56 (18)
N3—Co1—N1—C8	58.28 (17)	C14—C15—C16—C17	2.9 (3)
O2—Co1—N1—C9	124.52 (12)	Co1—O3—C17—C12	11.0 (3)
O6—Co1—N1—C9	−55.44 (12)	Co1—O3—C17—C16	−170.00 (12)
N2—Co1—N1—C9	30.62 (12)	C13—C12—C17—O3	−176.66 (18)
N3—Co1—N1—C9	−145.14 (12)	C11—C12—C17—O3	0.9 (3)
C1—O1—C2—C3	10.2 (3)	C13—C12—C17—C16	4.3 (3)
C1—O1—C2—C7	−170.3 (2)	C11—C12—C17—C16	−178.17 (17)
O1—C2—C3—C4	−179.9 (2)	O4—C16—C17—O3	−3.4 (2)
C7—C2—C3—C4	0.7 (3)	C15—C16—C17—O3	175.31 (17)
C2—C3—C4—C5	−0.3 (3)	O4—C16—C17—C12	175.75 (16)
C3—C4—C5—C6	0.7 (3)	C15—C16—C17—C12	−5.6 (3)
C4—C5—C6—C7	−1.4 (3)	C19—O5—C20—C21	−13.4 (3)
C4—C5—C6—C8	−170.7 (2)	C19—O5—C20—C25	167.15 (16)
Co1—O2—C7—C6	−35.5 (2)	O5—C20—C21—C22	−179.93 (18)
Co1—O2—C7—C2	146.84 (14)	C25—C20—C21—C22	−0.6 (3)
C5—C6—C7—O2	−175.95 (18)	C20—C21—C22—C23	−2.2 (3)
C8—C6—C7—O2	−6.4 (3)	C21—C22—C23—C24	1.9 (3)
C5—C6—C7—C2	1.7 (3)	C22—C23—C24—C25	1.0 (3)
C8—C6—C7—C2	171.31 (17)	C22—C23—C24—C26	−167.23 (18)
O1—C2—C7—O2	−3.0 (3)	Co1—O6—C25—C24	−24.4 (2)
C3—C2—C7—O2	176.47 (18)	Co1—O6—C25—C20	158.64 (13)
O1—C2—C7—C6	179.13 (17)	C23—C24—C25—O6	179.40 (17)
C3—C2—C7—C6	−1.4 (3)	C26—C24—C25—O6	−12.4 (3)
C9—N1—C8—C6	−151.49 (19)	C23—C24—C25—C20	−3.6 (3)
Co1—N1—C8—C6	3.0 (3)	C26—C24—C25—C20	164.64 (17)
C5—C6—C8—N1	−166.18 (19)	O5—C20—C25—O6	0.0 (2)
C7—C6—C8—N1	24.2 (3)	C21—C20—C25—O6	−179.45 (17)
C8—N1—C9—C10	106.4 (2)	O5—C20—C25—C24	−177.20 (16)
Co1—N1—C9—C10	−51.60 (16)	C21—C20—C25—C24	3.4 (3)
C11—N2—C10—C9	143.82 (18)	C27—N3—C26—C24	−161.12 (17)
Co1—N2—C10—C9	−27.56 (18)	Co1—N3—C26—C24	13.5 (3)
N1—C9—C10—N2	48.50 (19)	C25—C24—C26—N3	18.4 (3)
C10—N2—C11—C12	−175.28 (18)	C23—C24—C26—N3	−173.14 (18)
Co1—N2—C11—C12	−4.9 (3)	C26—N3—C27—C27^{i}	71.3 (2)
N2—C11—C12—C13	173.47 (19)	Co1—N3—C27—C27^{i}	−103.39 (19)
N2—C11—C12—C17	−4.1 (3)		

Symmetry code: (i) −*x*+1, −*y*+1, −*z*+1.

Hydrogen-bond geometry (Å, º)

D—H···*A*	*D*—H	H···*A*	*D*···*A*	*D*—H···*A*
C5—H5···N5*B*^{ii}	0.95	2.57	3.454 (19)	156

C9—H9*B*···O6	0.99	2.50	2.955 (2)	107
C18—H18*A*···N5*A*^{iii}	0.98	2.65	3.331 (10)	127
C27—H27*A*···O3^{i}	0.99	2.50	3.148 (2)	123
C27—H27*A*···O4^{i}	0.99	2.56	3.463 (2)	151
C27—H27*B*···O2	0.99	2.40	2.980 (2)	117
C28—H28*A*···O6	0.98	2.29	3.256 (3)	169
C30—H30*D*···N4	0.98	2.56	3.451 (5)	151

Symmetry codes: (i) −*x*+1, −*y*+1, −*z*+1; (ii) −*x*+2, −*y*, −*z*+1; (iii) *x*−1, *y*+1, *z*.